SÉRGIO HEITOR SOUSA FELIPE

SALT STRESS AND UV-B RADIATION MODULATE GROWTH, PHYSIOLOGY AND 20-HYDROXYECDYSONE CONTENTS IN BRAZILIAN-GINSENG [*Pfaffia glomerata* (SPRENG.) PEDERSEN]

Tese apresentada à Universidade Federal de Viçosa, como parte das exigências do Programa de Pós-Graduação em Botânica, para obtenção do título de *Doctor Scientiae*.

VIÇOSA
MINAS GERAIS - BRASIL
2019

Ficha catalográfica preparada pela Biblioteca Central da Universidade Federal de Viçosa - Câmpus Viçosa

T
F315s
2019

Felipe, Sérgio Heitor Sousa, 1986-
Salt stress and UV-B radiation modulate growth, physiology and 20-hydroxyecdysone contents in Brazilian-ginseng [*Pfaffia glomerata* (Spreng.) Pedersen] / Sérgio Heitor Sousa Felipe. – Viçosa, MG, 2019.
viii, 74 f. : il. (algumas color.) ; 29 cm.

Texto em inglês.
Orientador: Wagner Campos Otoni.
Tese (doutorado) - Universidade Federal de Viçosa.
Inclui bibliografia.

1. *Pfaffia glomerata*. 2. Ginseng. 3. Metabólitos. 4. Stresse (Fisiologia). 5. Radiação solar. I. Universidade Federal de Viçosa. Departamento de Biologia Vegetal. Programa de Pós-Graduação em Botânica. II. Título.

CDD 22. ed. 583.53

SÉRGIO HEITOR SOUSA FELIPE

SALT STRESS AND UV-B RADIATION MODULATE GROWTH, PHYSIOLOGY AND 20-HYDROXYECDYSONE CONTENTS IN BRAZILIAN-GINSENG [*Pfaffia glomerata* (SPRENG.) PEDERSEN]

Tese apresentada à Universidade Federal de Viçosa, como parte das exigências do Programa de Pós-Graduação em Botânica, para obtenção do título de *Doctor Scientiae*.

APROVADA: 26 de fevereiro de 2019.

Cleberson Ribeiro

Diego Silva Batista
(Coorientador)

Dimas Mendes Ribeiro

Márcia Adriana Carvalho dos Santos

Wagner Campos Otoni
(Orientador)

AGRADECIMENTOS

Agradeço incondicionalmente a Deus, pai todo poderoso, por tudo que tem realizado em minha vida;

Aos meus pais, Lourdes e Sebastião, ao meu padrasto Luciano, e aos meus irmãos Adriana e Neto pelo amor, carinho e apoio em todos os momentos;

À minha vó Celina (*in memoriam*);

Ao meu amor Vanessa Brito, pela amizade, amor, paciência e carinho;

À Universidade Federal de Viçosa (UFV) e Programa de Pós-Graduação em Botânica, pela valiosa oportunidade de crescimento profissional;

À CAPES (Coordenação de Aperfeiçoamento de Pessoal de Nível Superior), pela bolsa de estudo;

Ao meu orientador e amigo Prof. Dr. Wagner Otoni. Pela confiança, respeito, amizade e descomunal orientação durante todos os momentos e principalmente pelo exemplo como profissional e ser humano;

Ao meu coorientador e amigo Diego Batista, pelas discussões, conselhos e contribuições durante todo o desenvolvimento do trabalho;

Ao Prof. Dr. Fabio DaMatta pelas contribuições e sugestões apresentadas durante a construção desse trabalho;

Aos amigos e colegas do Laboratório de Cultura de Tecidos II pela colaboração direta nas análises experimentais e respeitoso convívio.

Aos amigos e colegas do Programa de Pós-Graduação em Botânica e do Laboratório de Anatomia Vegetal da UFV;

Ao amigo Dr. Camilo Vital pelo apoio durante as análises dos experimentos;

Aos técnicos do Núcleo de Biomoléculas da UFV pela oportunidade e acessibilidade;

A Dra. Noemi Leão e Dra. Ruth Linda, pesquisadoras da EMBRAPA, pela amizade, carinho e por terem sido responsáveis ao meu ingresso na pesquisa;

Aos amigos da EMBRAPA Elizabeth Shimizu, Alethéa Lisboa e Jorge de Almeida pela iniciação e estímulo à pesquisa;

A todos os funcionários e professores da UFV que de alguma forma contribuíram para minha formação acadêmica e profissional e a todos que de alguma forma fizeram parte desta conquista!

MUITO OBRIGADO!

BIOGRAFIA

SÉRGIO HEITOR SOUSA FELIPE, filho de Maria de Lourdes Sousa Felipe e Sebastião Sérgio Cabral Felipe, nasceu em 24 de agosto de 1986, na cidade de Soure, Ilha do Marajó, estado da Pará. Graduou-se em Agronomia em julho de 2010 pela Universidade Federal Rural da Amazônia. Iniciou o mestrado em Agronomia em agosto de 2012 na Universidade Federal Rural da Amazônia, tendo defendido tese em janeiro de 2015. Iniciou o doutorado em Botânica em março de 2015 na Universidade Federal de Viçosa, tendo defendido tese em fevereiro de 2019.

SUMÁRIO

ABSTRACT

FELIPE, Sérgio Heitor Sousa, D.Sc., Universidade Federal de Viçosa, February, 2019. **Salt stress and UV-B radiation modulate growth, physiology and 20-hydroxyecdysone contents in Brazilian-ginseng [*Pfaffia glomerata* (Spreng.) Pedersen]**. Adviser: Wagner Campos Otoni. Co-adviser: Diego Silva Batista.

The phytoecdysteroid 20-hydroxyecdysone (20E) is a secondary metabolite with high agrochemical, biotechnological and pharmacological potential, produced only by certain plant species. However, in relation to 20E, it is emphasized that: (i) the biosynthetic pathway is not fully elucidated in plants; (ii) it is not clear its real function in plants; (iii) there are few morphophysiological and molecular studies in plants that produce this metabolite; and (iv) there is a need to investigate the induction, biosynthesis, regulation and translocation of this metabolite in plants. In this sense, two experiments were performed aiming to evaluate the impact of salt stress and UV-B radiation on growth, physiology, expression of key genes involved in the biosynthesis and the 20E content in *Pfaffia glomerata*. In the first experiment, accession 43 (A43) plants with 40-day-old grown in greenhouse were exposed to 0-, 120-, 240-, 360- and 480-mM sodium chloride (NaCl) for 11 consecutive days. In the second experiment, two accessions (A22 and A43) plants with 20-day-old grown in *in vitro* were exposed to 0-, 2- and 4-h UV-B radiation for 20 consecutive days. Mild salt stress (i.e., 120 mM NaCl) increased 20E concentrations in the leaves (47%) relative to the control, with no significant effect on photosynthesis and biomass accumulation. In contrast, plants under severe salt stress (i.e., 240 to 480 mM NaCl) did not increase 20E concentrations compared to the control. Additionally, severe salt stress caused marked damage in biomass accumulation and photosynthetic performance in parallel with the nutritional imbalance. To combat severe salt stress, *P. glomerata* plants displayed an increase in salicylic acid levels, antioxidant enzyme activities and osmoregulatory status (e.g., glucose, fructose, total amino acids, and proline). UV-B radiation differentially impacted the accessions A22 and A43. In A22, 4 h of exposure reduced biomass accumulation and electron transport rate, on the other hand, increased antioxidant activity (e.g., peroxidases), while A43 did not vary for these characteristics. Besides, only A22 increased the 20E concentration

under 2 and 4 h of UV-B in leaves (28 and 21%, respectively) and roots (16 and 13%, respectively). This contrasting performance between A22 and A43 to UV-B radiation can be explained by A43 displayed 56% more anthocyanin to the former, a possible defense against UV-B. In both experiments, the production of 20E was accompanied by an upregulation of *Spook* and *Phantom* genes. The results of this work bring an unprecedented better understanding of the 20E regulation under conditions of abiotic stresses (salt stress and UV-B radiation). Finally, we provide findings that can be applied to increase 20E levels and contribute to the development of biotechnology, pharmacology and *ex vitro* and *in vitro* culture of the species.

RESUMO

FELIPE, Sérgio Heitor Sousa, D.Sc., Universidade Federal de Viçosa, fevereiro de 2019. **Estresse salino e radiação UV-B modula crescimento, fisiologia e teor de 20-hidroxiecdisona em Ginseng-brasileiro [*Pfaffia glomerata* (Spreng.) Pedersen]**. Orientador: Wagner Campos Otoni. Coorientador: Diego Silva Batista.

O fitoecdisteroide 20-hidroxiecdisona (20E) é um metabólito secundário com elevado potencial agroquímico, biotecnológico e farmacológico, produzido somente por determinadas espécies de plantas. Contudo, em relação ao 20E, destaque-se que: (i) a sua via biossintética não está totalmente elucidada em plantas; (ii) não se sabe a sua real função em plantas; (iii) há escassez de estudos morfofisiológico e moleculares em plantas produtoras desse metabólito; e ainda, (iv) há necessidade de se investigar a indução, biossíntese, regulação e translocação desse metabólito em plantas. Nesse sentido, dois experimentos foram realizados com o objetivo de avaliar o impacto do estresse salino e da radiação UV-B sobre o crescimento, a fisiologia e a expressão de genes ligados à biossíntese e teor de 20E em *Pfaffia glomerata*. No primeiro experimento, plantas do acesso 43 (A43), com 40 dias de cultivo em casa de vegetação, foram expostas à 0, 120, 240, 360 e 480 mM de cloreto de sódio (NaCl), durante 11 dias consecutivos. No segundo experimento, plantas de dois acessos (A22 e A43), com 20 dias de cultivo *in vitro*, foram expostas à 0, 2 e 4 h de radiação UV-B, durante 20 dias consecutivos. O estresse salino leve (120 mM de NaCl) promoveu aumento de 20E nas folhas (47%) em relação ao controle, sem efeito significativo na fotossíntese e no acúmulo da biomassa. Em contraste, plantas sob estresse salino severo (240 a 480 mM de NaCl) não aumentaram as concentrações de 20E em comparação ao controle. Adicionalmente, o estresse salino severo causou acentuados prejuízos no acúmulo de biomassa e desempenho fotossintético em paralelo com o desequilíbrio nutricional. Para combater o estresse salino severo, plantas de *P. glomerata* aumentaram os níveis de ácido salicílico, atividades das enzimas antioxidantes e a osmorregulação (p.ex., glicose, frutose, aminoácidos totais e prolina). A radiação UV-B impactou diferencialmente os acessos A22 e A43. No A22, 4 h de exposição à UV-B reduziu a biomassa e taxa de transporte de elétrons, por outro lado, aumentou a atividade antioxidante (p.ex., peroxidases), enquanto o

A43 não variou para essas características. Além disso, somente o A22 aumentou a concentração de 20E sob 2 e 4 h de UV-B nas folhas (28 e 21%, respectivamente) e raízes (16 e 13%, respectivamente). Esse desempenho contrastante entre A22 e A43 à radiação UV-B podem ser explicados pelo fato de o A43 ter 56% a mais de antocianina em comparação ao A22, uma possível defesa contra UV-B. Em ambos os experimentos, a produção de 20E foi acompanhada pela regulação positiva dos genes *Spook* e *Phantom*. Os resultados deste trabalho fornecem de forma inédita um melhor entendimento da regulação da produção de 20E sob condições de estresses abióticos (estresse salino e radiação UV-B). Por último, essas informações poderão ser aplicadas para aumentar os níveis de 20E e contribuir para o desenvolvimento da biotecnologia, farmacologia e cultivo *ex vitro* e *in vitro* da espécie.

INTRODUCTION

Plants have the ability to biosynthesize a high diversity of secondary metabolites, which are capable of acting, directly or indirectly, in different morphophysiological processes when dealing with highly complex biotic (e.g., insects, fungi and bacteria) and/or abiotic (e.g., light, temperature and water availability) interactions (Fang *et al*., 2019). These secondary plant metabolites can be subdivided into terpenes, phenolics and nitrogen, sulphur comprising compounds, depending on the biosynthetic pathways (Jamwal *et al*., 2018). The terpene pathway produces several metabolites with pharmacological and pesticidal purposes (Tetali, 2018), as particularly the phytoecdysteroid 20-hydroxyecdysone (20E), which is found in some species of plants with agrochemical, biotechnological, pharmacological and medicinal potential (Fesctucci-Buselli *et al*., 2008a).

Ecdysteroids (ECDs) are classified as steroidal hormones encountered in arthropods that intervene on the ecdysis process (zooecdysteroids – ZEs), but can also be found in organisms that are not part of the Arthropoda Phylum, including plant species (phytoecdysteroids – PEs) (Chaubey, 2018). Furthermore, although ECDs are not biosynthesized by mammals, they have medicinal effects (Dinan, 2001; Báthori and Pongracz, 2005; Dinan and Lafont, 2006; Mallek *et al*., 2018; Phungphong *et al*., 2018). The 20E molecule is the main hormone associated with the process of ecdysis in insects, whereas in plants it is considered a secondary metabolite (Cao *et al*., 2018; John *et al*., 2018).

In *Arabdopsis thaliana*, phytosterols biosynthesis may occur by lanosterol pathway (main sterol pathway in insects) and/or cycloartenol (main phytosterols pathway in plants) (Ohyama *et al*., 2009). For spinach (*Spinacia oleracea*), a 20E-producing species, it has been suggested that biosynthesis occurs from the mevalonic acid pathway, including lathosterol, cholesterol, ecdysone, 2-deoxy-20-ecdysone and 2-deoxy-20-hydroxyecdysone (Adler and Grebenok, 1999). These same authors suggest that lathosterol may be the direct precursor of 20E. However, the biosynthetic 20E pathway in plants is not fully elucidated and has many gaps (Festucci-Buselli *et al*., 2008a, Boo *et al*., 2013; Tsukagoshi *et al*., 2016); thus, it is necessary to investigate genes that are related to lanosterol and cycloartenol pathways in plants (Fig. 1).

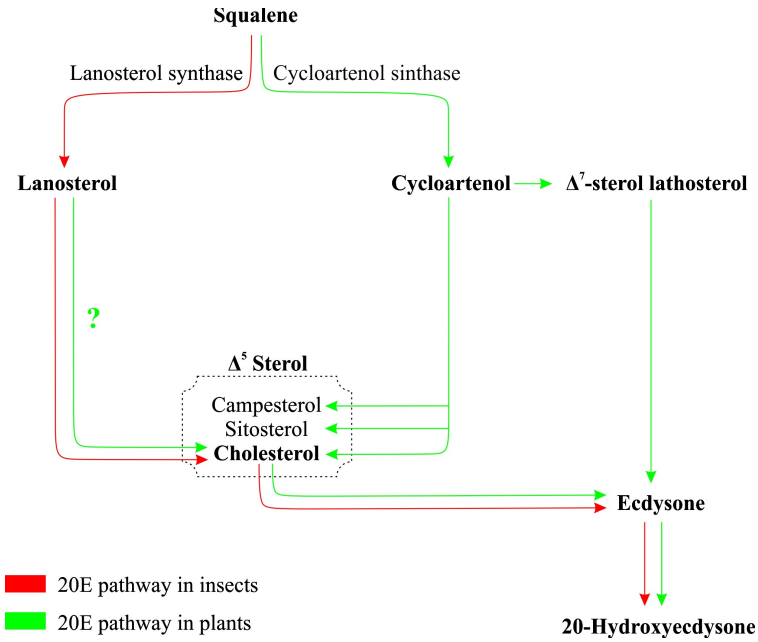

Figure 1. Simplified biosynthetic pathway of 20E in plants (adapted from Adler and Grebenok, 1999; Bakrim *et al*., 2008; Ohyama *et al*., 2009; Tarkowská and Strnad, 2016).

Among the 20E-producing plants, there is the *Pfaffia glomerata* (Spreng.) Pedersen (Amaranthaceae), which is extensively used in traditional medicine (Lorenzi and Matos, 2002). Several pharmacological studies have shown its positive results when treating gastric issues (Freitas *et al*., 2004, Mazzeo *et al*., 2013); besides an anti-inflammatory and analgesic action (Neto *et al*., 2005) and antioxidant (Souza Daniel *et al*., 2005), in addition to an antimicrobial action as an adjuvant in the control of dental cavities (Moura *et al*., 2011).

P. glomerata has different compounds identified as glomeric acid, pfameric acid, rubrosterone, 20-hydroxyecdysone, ecdysterone and *β*-D glucopyranosyl oleate (Shiobara *et al*., 1993). Moreover, the presence of 20E contents is reported in flowers, leaves, stems and roots throughout the plant growth and development, with roots registering the its highest concentration (Festucci-Buselli *et al*., 2008b). As for the roots of the genus *Pfaffia*, the plant's main organ in terms of usage in traditional medicine and research, their main isolated compounds are stigmasterol, sitosterol and allantoin, in addition to the aforementioned compounds that are part of the ecdysteroid, triterpenoid and nortriterpenoid classes (Nakai *et al*., 1984; Nishimoto *et al*., 1984).

Our research group designated as Núcleo de Prospecção Botânica, Fitoquímica e Gênica (*Botanical, Phytochemical and Genetics Prospection Nucleus*)

of the Federal University of Viçosa has been conducting studies with *P. glomerata* since 2002, the year when the installation of an *in vitro* germplasm bank of the Plant Tissue Culture Laboratory of the Federal University of Viçosa began in a consortium with Embrapa Recursos Genéticos e Biotecnologia (*Embrapa Genetic Resources and Biotechnology*), with a total of 71 accessions collected in the Brazilian states of Mato Grosso do Sul and Paraná (Kamada, 2006). Since then, different studies have been conducted to foster the increase of 20E, as well as the analysis and characterization of plants that produce this metabolite.

We have recently developed a pioneering transcriptome study in *P. glomerata* (Batista *et al*., 2018), generating new perspectives for the analysis of genes which may be an element of the 20E biosynthetic pathway. Thus, determining elicitors and mechanisms that can induce the 20E production in *P. glomerata* is the key point for the analysis of genes linked to the biosynthesis of this molecule, as well as to generate new perspectives and to enable a better understanding of its function and mode of action in plants.

Among the potential strategies that may be explored to induce changes in the secondary metabolism of plants, there is the application of salt stress and UV-B radiation. Nevertheless, changes in secondary metabolism may happen positively, negatively and transiently, depending on the intensity and time of exposure (Naik and Al–Khayri, 2016).

Ultraviolet (UV) radiation can be classified into three types according to the wavelength: UV-A (400–320 nm), UV-B (320–280 nm) and UV-C (280–100 nm). In plant morphogenesis, UV-B can induce different changes such as increased leaf thickening, petioles shortening, winding and changes in leaf shape and width. However, the phenotype induced by UV-B is diverse, with many apparently contradictory reports on plant architecture (Robson *et al*., 2015). Also, buckwheat (*Fagopyrum esculentum*) plants with higher anthocyanin content showed greater resistance to the harmful effects of UV-B radiation (Dębski *et al*., 2016). In this sense, the evaluation of contrasting plants of the same species in the production of anthocyanin under UV-B radiation can be an interesting strategy to induce changes in the secondary metabolism of plants and, consequently, evidence possible relations of this metabolic change with the plants' ability to present higher (high anthocyanin content) or lower (low anthocyanin content) photoprotection on exposure to UV-B.

In salt stress, plants respond to this stimulus because of the deficiency in the water absorption caused by the decrease of the osmotic potential and by the accumulation of salts inside the plant (Munns and Tester, 2008). Study involving the induction of salt stress in cotton (*Gossypium hirsutum*) plants evidenced changes in secondary metabolism promoting the increase of gossypol, flavonoids and tannic acid contents (Wang *et al*., 2015). However, few information is available on how salinity affects secondary plant defense compounds (Ballhorn *et al*., 2011; Ballhorn and Elias, 2014).

Here, we evaluate the effect of salt stress and UV-B radiation on the growth performance, physiology features and biosynthesis of 20E *in P. glomerata*, in order provide a better understanding on the relationship between these abiotic effects and the regulation of the production of 20E.

REFERENCES

Adler JH, Grebenok, RJ (1999) Occurrence, biosynthesis, and putative role of ecdysteroids in plants. Crit Rev Biochem Mol Biol 34(4): 253–264.

Bakrim A, Maria A, Sayah F, Lafont R, Takvoriam N (2008) Ecdysteroids in spinach (*Spinacia oleracea* L.): Biosynthesis, transport and regulation of levels. Plant Physiol Biochem 46(10):844–854.

Ballhorn DJ, Elias JD (2014) Salinity-mediated cyanogenesis in white clover (*Trifolium repens*) affects trophic interactions. Ann Bot 114(2):357–366.

Ballhorn DJ, Kautz S, Jensen M, Schmitt I, Heil M, Hegeman AD (2011) Genetic and environmental interactions determine plant defences against herbivores. J Ecol 99(1):313–326.

Báthori M, Pongrácz Z (2005) Phytoecdysteroids-from isolation to their effects on humans. Curr Med Chem, 12(2):153–172.

Batista DS, Koehler AD, Romanel VC, Souza VC, Silva TD, Almeida MC, Maciel TEF, Bueno PR, Felipe SHS, Saldanha CW, Maldaner J, Carnevalli LL, Festucci-Buselli RA, Otoni WC (2018) *De novo* assembly and transcriptome of *Pfaffia glomerata* uncovers the role of photoautotrophy and the P450 family genes in 20-hydroxyecdysone production. Protoplasma 1–14.

Boo KH, Lee D, Nguyen QV, Jin SB, Kang S, Viet CD, Park SP, Lee D-S, Riu KZ, (2013) Fluctuation of 20-hydroxyecdysone in individual organs of *Achyranthes japonica* during reproductive growth stage and its accumulation into seed. J Korean Soc Appl Biol Chem 56:b335–338.

Cao VD, Riu KZ, Boo KH (2018) Biosynthesis and accumulation of 20-hydroxyecdysone in individual male and female spinach plants during the reproductive stage. Plant Physiol Biochem 129:394–399.

Chaubey, MK (2018) Role of phytoecdysteroids in insect pest management: a review. J Agron 17(1):1–10.

Dębski H, Szwed M, Wiczkowski W, Szawara-Nowak D, Bączek N, Horbowicz M (2016) UV-B radiation increases anthocyanin levels in cotyledons and inhibits the growth of common buckwheat seedlings. Acta Biol Hung 67(4):403–411.

Dinan L (2001) Phytoecdysteroids: biological aspects. Phytochemistry 57(3):325–339.

Dinan L, Lafont R (2006) Effects and applications of arthropod steroid hormones (ecdysteroids) in mammals. J Endocrinol 191(1):1–8.

Fang C, Fernier AR, Luo J (2019) Exploring the diversity of plant metabolism. Trends Plant Sci 24(1):83–98.

Festucci-Buselli RA, Contim LAS, Barbosa LCA, Stuart JJ, Otoni WC (2008a) Biosynthesis and potential functions of the ecdysteroid 20-hydroxyecdysone – a review. Botany 86(9):978-987.

Festucci-Buselli RA, Contim LA, Barbosa LCA, Stuart JJ, Vieira RF, Otoni WC (2008b) Level and distribution of 20-hydroxyecdysone during *Pfaffia glomerata* development. Braz J Plant Physiol 20(4):305–311.

Freitas CS, Baggio CH, Da Silva-Santos JE, Rieck L, De Moraes Santos CA, Correa JRC, Ming LC, Cortez DAG, Marques MCA (2004) Involvement of nitric oxide in the gastroprotective effects of an aqueous extract of *Pfaffia glomerata* (Spreng) Pedersen, Amaranthaceae, in rats. Life Sci 74(9):1167–1179.

Jamwal K, Bhattacharya S, Puri S (2018) Plant growth regulator mediated consequences of secondary metabolites in medicinal plants. Journal of applied research on medicinal and aromatic plants. J Appl Res Med Aromat Plants 9:26–38.

John R, Shajitha PP, Devassy A, Mathew L (2018) Effect of elicitation and precursor feeding on accumulation of 20-hydroxyecdysone in *Achyranthes aspera* Linn. cell suspension cultures. Physiol Mol Biol Plants 24(2):275–284.

Kamada T (2006) Avaliação da diversidade genética de populações de fáfia (*Pfaffia glomerata* (Spreng.) Pedersen) por RAPD, caracteres morfológicos e teor de beta-ecdisona. Tese de doutorado, Universidade Federal de Viçosa, Viçosa, MG, Brazil. Available in: http://locus.ufv.br/handle/123456789/1298

Lorenzi H, Matos FJA (2002) Plantas medicinais do Brasil: nativas e exóticas. Nova Odessa: Instituto Plantarum pp. 5–46.

Mallek A, Movassat J, Ameddah S, Liu J, Semiane N, Khalkhal A, Dahmani Y (2018) Experimental diabetes induced by streptozotocin in the desert gerbil, *Gerbillus gerbillus*, and the effects of short-term 20-hydroxyecdysone administration. Biomed Pharmacother 102:354–361.

Mazzeo GCCS, Cortez FS, Pusceddu FH, Santos AR, Guimarães LL, Amaral FP, Silva MPO, Toma W (2013) Avaliação da atividade antiulcerogênica e ecotoxicológica do extrato hidroalcoólico 70% obtido a partir das folhas de *Pfaffia glomerata* (Spreng.) Pedersen (Amaranthaceae). UNISANTA BioSci 2(2):75–80.

Moura CL, Casemiro LA, Martins CHG, Cunha WR, Silva MLA, Cury AHV (2011) Evaluation of the antimicrobial activity of the plant species *Pfaffia glomerata* against oral pathogens. R Invest 11(2):24–28.

Munns R, Tester M (2008) Mechanisms of salinity tolerance. Annu Rev Plant Biol 59:651–681.

Nakai S, Takagi N, Miichi H, Hayashi S, Nishimoto N, Takemoto T, Kizu H (1984) Pfaffosides, nortriterpenoid saponins, from *Pfaffia paniculata*. Phytochemistry 23(8):1703–1705.

Neto AG, Costa JMLC, Belati C, Vinholis AHC, Possebom LS, Da Silva Filho AA, Cunha WR, Carvalho JCT, Bastos JK, Silva MLA (2005) Analgesic and anti-inflammatory activity of a crude root extract of *Pfaffia glomerata* (Spreng.) Pedersen. J Ethnopharmacol 96(1):87–91.

Nishimoto N, Nakai S, Takagi N, Hayashi S, Takemoto T, Odashima S, Kizu H, Wada Y (1984) Pfaffosides and Nortriterpenoid Saponins from *Pfaffia paniculata*. Phytochemistry 23:139–142.

Ohyama K, Suzuki M, Kikuchi J, Saito K, Muranaka T (2009) Dual biosynthetic pathways to phytosterol via cycloartenol and lanosterol in *Arabidopsis*. Proc Natl Acad Sci 106:725–730.

Phungphong S, Kijtawornrat A, Chaiduang S, Saengsirisuwan V, Bupha-Intr T (2017) 20-Hydroxyecdysone attenuates cardiac remodeling in spontaneously hypertensive rats. Steroids 126:79–84.

Robson T, Klem K, Urban O, Jansen MA (2015) Re-interpreting plant morphological responses to UV-B radiation. Plant Cell Environ 38(5):856–866.

Shiobara Y, Inque SS, Keato K, Nishigushi Y, Oishi Y, Nishimito N, Oliveira F, Aksue G, Akisue MK, Hashimoto GA (1993) A nortriterpenoid, triterpenoid and ecdysteroids from *Pfaffia glomerata*. Phytochemistry 32(6):1527–1530.

Souza Daniel JF, Alves KZ, Silva Jacques D, Silva e Souza PV, Carvalho MG, Freire RB, Ferreira DT, Freire MFI (2005) Free radical scavenging activity of *Pfaffia glomerata* (Spreng.) Pederson (Amaranthaceae). Indian J Pharmacol 37(3):174–178.

Tarkowská D, Strnad M (2016) Plant ecdysteroids: plant sterols with intriguing distributions, biological effects and relations to plant hormones. Planta 244(3):545–555.

Tetali, SD (2018) Terpenes and isoprenoids: a wealth of compounds for global use. Planta. Available online in: https://doi.org/10.1007/s00425-018-3056-x

Tsukagoshi Y, Ohyama K, Seki H, Akashi T, Muranaka T, Suzuki H, Fujimoto Y (2016) Functional characterization of CYP71D443, a cytochrome P450 catalyzing C-22 hydroxylation in the 20-hydroxyecdysone biosynthesis of *Ajuga* hairy roots. Phytochemistry 127:23–28.

Wang Q, Eneji AE, Kong X, Wang K, Dong H (2015) Salt stress effects on secondary metabolites of cotton in relation to gene expression responsible for aphid development. PloS One 10(6):e0129541.

CHAPTER 1

Mild salt stress does not alter growth, ion balance and photosynthetic performance but enhances 20-hydroxyecdysone contents in Brazilian-ginseng [*Pfaffia glomerata* (Spreng.) Pedersen]

Abstract

Salt stress is a major threat to agriculture. However, depending on the stress intensity, increased secondary metabolite levels can occur with no major damages to plant growth and development. The phytoecdysteroid (PE) 20-hydroxyecdysone (20E) is a secondary metabolite with biotechnological, medicinal, pharmaceutical and agrochemical applicability. We tested the hypothesis that salt stress increases the 20E content in *Pfaffia glomerata*. 40-day-old plants grown in greenhouse were exposed to 0, 120, 240, 360 or 480 mM of sodium chloride (NaCl) for 11 days. Mild salt stress (i.e., 120 mM of NaCl) led to increased 20E concentrations in leaves (47%) relative to the control with no significant effect on photosynthesis and biomass accumulation, thus allowing improved 20E contents on a per whole-plant basis. In contrast, plants under high salt stress (i.e., 240 to 480 mM of NaCl) displayed similar 20E concentrations in leaves compared to the control, but with marked impairments to biomass accumulation and photosynthetic performance (coupled with decreased sucrose and starch levels) in parallel to nutritional imbalance. Severe salt stress also strongly increased salicylic acid levels, antioxidant enzyme activities, and osmoregulatory status. Regardless of stress severity, 20E production was accompanied by the upregulation of *Spook* and *Phantom* genes. Our findings suggest that *P. glomerata* cultivation in low salinity soils can be considered as a suitable agricultural option to increase 20E levels, since metabolic and structural complexity that makes its artificial synthesis very difficult.

Keywords: abiotic stress, Brazilian-ginseng, Halloween genes, photosynthesis, phytoecdysteroid, salt stress.

Introduction

Plants are often exposed to several environmental stresses such as drought, waterlogging, temperature extremes and salinity. Salinity affects the soils of more than 100 countries (≅ 1 billion ha of land area) and contributes to the degradation of land and water resources (FAO and ITPS, 2015). Salt stress affects plants in two distinct ways, by inducing osmotic stress causing ion toxicity due to the accumulation of sodium (Na^+) and/or chloride (Cl^-) at toxic concentrations, thus limiting nutrient absorption (e.g., K^+ and Ca^{2+}) and disturbing the ionic balance (Almeida *et al*., 2017; Assaha *et al*., 2017; Wangsawang *et al*., 2018). As general consequences of these imbalances plant growth and productivity can be severely impaired (Hanin *et al*., 2016; Acosta-Motos *et al*., 2017; Negrão *et al*., 2017).

Overall, plants cope with reductions in soil osmotic potential (osmotic or water-deficit stress) caused by salinity via acclimation mechanisms such as osmotic adjustment and maintenance of cell turgor, which are associated with increases in the levels of solutes such as amino acids (e.g., proline), quaternary ammonium compounds (e.g., glycine betaine), tertiary sulfonium compounds (e.g., dimethylsulfoniopropionate), polyols (e.g., mannitol), and soluble sugars (e.g., fructose, trehalose, and raffinose) (Reis *et al*., 2012; Richter *et al*., 2015; Farhangi-Abriz and Torabian, 2018). The ionic imbalance caused by salinity can disrupt the metabolic homeostasis, which in turn can promote the reactive oxygen species (ROS) formation at levels detrimental to cells (e.g., superoxide anion ($O_2^{\bullet-}$), singlet oxygen ($^1O_2$), hydroxyl radical ($^{\bullet}OH$), and hydrogen peroxide (H_2O_2)) (Azevedo-Neto *et al*., 2006; Miller *et al*., 2010; Hossain *et al*., 2017), provoking serious damages to the metabolism through the oxidation of lipids, nucleic acids and proteins (Gill and Tuteja, 2010). To cope with salt-induced oxidative stress, plants evolved a sophisticate mechanism encompassing both enzymatic (e.g., superoxide dismutase (SOD), catalase (CAT) and ascorbate peroxidase (APX)) (Koleška *et al*., 2017; Vighi *et al*., 2017; Farhangi-Abriz and Torabian, 2018) and non-enzymatic (e.g., ascorbic acid (ASC), reduced glutathione (GSH), and α-tocopherol) systems (Chakraborty *et al*., 2016; Arora and Bhatla, 2017; Kaur *et al*., 2017).

The deleterious effects of salinity caused by osmotic stress, nutritional imbalance, and oxidative stress ultimately promote decreases in leaf area, chlorophyll content, stomatal conductance and photosystem II (PS II) efficiency,

which collectively lead to decreased photosynthetic performance on a leaf- and whole-plant scales (Meloni *et al*., 2003; Chaves *et al*., 2009; Kan *et al*., 2017; Çiçek *et al*., 2017). Nevertheless, salt stress can induce the biosynthesis of molecules from secondary metabolism with high biotechnological interest in plants (Wahid and Ghazanfar, 2006; Akula and Ravishankar, 2011; Wang *et al*., 2015; Abdallah *et al*., 2016; Yadav *et al*., 2017). Consequently, the understanding on how salt stress can lead to increased levels of metabolites with biotechnological, medicinal, pharmaceutical and agrochemical applicability is of utmost importance and may contribute to the development of agriculture under unfavorable conditions.

Plants have developed several genetic mechanisms that produce secondary metabolites, which play important roles in defense and acclimatation to face biotic and/or abiotic stresses (Barton and Boege, 2017). Here, we stand out the 20-hydroxyecdysone (20E), the main hormone related to ecdysis process in insects (zooecdysteroid), but acting as a secondary metabolite (phytoecdysteroid) in the plant kingdom. The 20E displays potential therapeutic applications (John *et al*., 2018), and it is produced in relatively large amounts in some species such as *Pfaffia glomerata* (Spreng.) Pedersen (Amaranthaceae).

P. glomerata is a medically and economically important species with proven phytotherapeutic properties (Almeida *et al*., 2017; Silva *et al*., 2017; Dias *et al*., 2019; Vardanega *et al*., 2019). It has been demonstrated that application of 20E protects *Triticum aestivum* plants from oxidative imbalance, enhances the anti-oxidative systems and improves resistance to lead stress (Lamhamdi *et al*., 2016), in addition to enhancing tolerance to salt stress (Li *et al*., 2018). In *P. glomerata*, recent information has revealed two Halloween genes – *Spook* (*Spo*) and *Phantom* (*Phm*) – associated with 20E biosynthesis (Batista *et al*., 2018), although the 20E biosynthetic pathway is not fully elucidated (Festucci-Buselli *et al*., 2008a; Ohyama *et al*., 2009; Tsukagoshi *et al*., 2016); in addition, the role of 20E is also poorly understood (Festucci-Buselli *et al*., 2008a; Boo *et al*., 2013; Thussagunpanit *et al*. 2017). Thus, the use of experimental strategies to analyze genes involved in 20E biosynthesis may provide a better understanding of the ecological, physiological and biochemical role in plants (Festucci-Buselli *et al*., 2008b).

Given the facts described above, we hypothesized that salt stress, depending on its severity, can lead to increased 20E contents (absolute amounts) in *Pfaffia glomerata*. Here, we firstly characterize the responses of *P*. *glomerata* to salt stress

and, secondly, examine the production of 20E as affected by salinity. We demonstrate that mild salinity does not affect plant growth and photosynthesis but is able to increase the total 20E production on a per plant basis. Our study offers, therefore, novel insights on how *P. glomerata* deals with salt stress and explore underlying mechanisms by which 20E production is affected by salinity.

Materials and methods

Plant growth and experimental design

Plants of *Pfaffia glomerata* (accession 43) used in this study were taken from the Germplasm bank of the Plant Tissue Culture Laboratory (Federal University of Viçosa, Brazil), where 71 accessions are maintained *in vitro*. Voucher material was deposited at the Leopoldo Krieger Herbarium (UFJF, Juiz de Fora, MG, Brazil) under the code number CESJ 63317.

Explants with a nodal segment (1.5 cm) were cultured in test tubes (22 mm diameter x 150 mm height) containing 10 mL Murashige and Skoog (1962) medium supplemented with MS vitamins, 100 mg L^{-1} myo-inositol and 3% sucrose (w/v), pH was adjusted to 5.7 ± 0.1, solidified with 5.5 g L^{-1} agar (Phytotechnology Laboratories, LLC, Shawnee Mission, KS, USA) and sterilized by autoclaving at 121 °C and 1.5 atm for 20 min. The plants were cultivated for 40 days under 25 ± 2 °C, with 40 µmol m^{-2} s^{-1} of irradiance and 16-h photoperiod.

After the *in vitro* culture, plants were acclimatized for 10 days in 300-mL plastic cups (COPOBRAS, São Ludgero, SC, Brazil). Then, they were transplanted to plastic vessels (24 x 21 x 15 cm; EME-A-EME Ind. Com. Ltda., Petrópolis, RJ, Brazil) filled with 2 kg of commercial substrate Tropstrato HT® (Vida Verde, Mogi Mirim, SP, Brazil) and then the plants were grown in a greenhouse (average temperature 27.5 ± 2°C; natural light conditions with intensity of ~750 µmol photons m^{-2} s^{-1}). During the greenhouse cultivation (51 days total, being 40 days of growth without salt and 11 days with salt), the plants were fertilized at 15 and 30 days with 5.5 g NPK - 26:06:12 (Polyblen Montanha®, São Paulo, SP, Brazil).

Salt treatments 0 (control), 120, 240, 360 and 480 mM of sodium chloride (NaCl; ACS reagent, ≥ 99%, Sigma-Aldrich, St. Louis, MO, USA) were applied to 40-day-old plants during 11 days. After this period, samplings and measurements were performed. Plants were irrigated during the experiment using deionized water (conductivity equal to 0.04 mS). The volume of irrigation water was applied to maintain the soil near field capacity. The experimental design was completely randomized with 7 replicates; the experimental unit was one plant per vessel.

Growth parameters

Plant tissues were collected at the end of the experiment and separated into root, stem, and leaves, after which they were oven-dried at 50 °C for 72 h to obtain the dry weight (DW). The abscised leaves were collected and their masses included in total plant DW. Plant height was also assessed.

Tissue nutrient analysis

Leaves were sliced and dried at 50 °C with forced and continuous ventilation until the dry mass stabilized and then were milled (using a Knife Mill, Willey®). To quantify the levels of P, K^+, Ca^{2+}, Mg^{2+}, S, Zn, Cu, Mn, Fe and Na^+, the leaf samples were submitted to nitric-perchloric digestion (4:1) (v/v) and the N the digestion was sulfuric by Kjeldahl method (Sarruge and Haag, 1974). Determination of P was by colorimetry through the ascorbic acid with reading in molecular absorption spectrophotometer (Femto Indústria e Comércio de Instrumentos Ltda., São Paulo, SP, Brazil); K and Na by flame photometry (Corning 400, Corning Inc., NY, USA); Ca, Mg, Fe, Cu, Zn and Mn by atomic absorption spectrophotometry (Mulgrave, Victoria, Australia); and S by turbidimetry as reported in Alvarez *et al*. (2001).

Leaf gas exchange and chlorophyll a *fluorescence*

Gas exchange analyzes were performed on the third fully expanded leaf from the apex of plants using the open gas exchange system Li-6400XT (Li-Cor, Lincoln, NE, USA) equipped with an integrated fluorescence chamber heads (Li-6400-40, Li-Cor, USA). The net CO_2 assimilation rate (A), stomatal conductance to water vapor (g_s), transpiration rate (E) and internal CO_2 concentration (C_i) were measured from 08:30 to 12:00 hours under an external CO_2 concentration of 400 μmol mol^{-1} air and average temperature of 25 ºC. All measurements were conducted under an artificial, saturating light of 1000 μmol m^{-2} s^{-1} that was provided by a light-emitting diode with 10 % blue light in order to maximize stomata opening.

Previously dark-adapted (8 h) leaf tissues were illuminated with weak modulated measuring beams (0.03 μmol m^{-2} s^{-1}) to obtain the initial fluorescence (F_0). Saturating white light pulses (8,000 μmol m^{-2} s^{-1}; 0.8 s) was applied to ensure maximum fluorescence emissions (F_m), from which the variable-to-maximum Chl fluorescence ratio, $F_v/F_m=[(F_m-F_0)/F_m)]$, was calculated. The coefficient for photochemical quenching (qP) was calculated as $qP=(F_m'-F_s)/(F_m'-F_0')$ and that for

non-photochemical quenching (NQP) was calculated as NQP=(F_m/F_m')-1. The actual quantum yield of PS II electron transport (Φ_{PSII}) was computed as $\Phi_{PSII}=(F_m'-F_s)/F_m'$). The apparent electron transport rate (ETR) was estimated as ETR= Φ_{PSII}*PPFD*f*α where f is a factor that accounts for the partitioning of energy between PS II and PSI and is assumed to be 0.5, which indicates that excitation energy is distributed equally between the two photosystems, and α is the leaf absorptance by photosynthetic tissues and is assumed to be 0.84 (Maxwell and Johnson, 2000).

Determination of total chlorophyll and quantification carbohydrates, protein and amino acid levels

Leaf samples (third fully expanded leaf from the apex of plants), collected at the end of the experiment at 13:00 hours, were flash frozen in liquid nitrogen, and subsequently ground and lyophilized for analysis. Approximately 30 mg lyophilized tissues were used for extraction with ethanol as described by Praxedes *et al*. (2006). Photosynthetic pigments were determined as described by Arsovski *et al*. (2018). Carbohydrates (starch, sucrose, glucose, and fructose) were assessed as described by Fernie *et al*. (2001). Protein and total amino acid levels were analyzed as reported in Cross *et al*. (2006).

Proline content

Proline content was determined following Bates *et al*. (1973), with minor modifications. Approximately 10 mg of lyophilized leaf tissue (third fully expanded leaf from the apex of plants) were suspended in 1 mL of 3% sulfosalicylic acid (w/v), vortexed (2 times for 20 s) and centrifuged at 6,300 *g* for 10 min. Later, 200 µL of the supernatant was collected, 400 µL of acidic ninhydrin solution (1.25 g of ninhydrin, 30 mL of glacial acetic acid and 20 mL of 6 M phosphoric acid) were added and the samples were incubated at 100 °C for 1 h. The reaction was stopped in an ice bath. Then, readings were made at 520 nm and a calibration curve was obtained by preparing proline standard solutions (0 to 220 µg mL^{-1}; Sigma-Aldrich, St. Louis, MO, USA) and expressed in mmol mg^{-1} dry weight (DW).

Quantification of polyamines and phytohormones

The quantification was performed according to Napoleão *et al*. (2017). Approximately 110 mg of fresh leaf tissue (third fully expanded leaf from the apex of plants) were ground in liquid nitrogen followed of extraction by twice with 400 µL of methanol: isopropanol: acetic acid (20:79:1; v/v/v). The samples were vortexed (4 times for 20 s), sonicated (10 min), kept on ice (30 min), centrifuged (20,000 *g*, 10 min at 4 °C), and the supernatant was collected. Then, the supernatant was filtered (Econofltr PVDF 13 mm and 0.2 µm; Agilent Technologies, Santa Clara, CA, USA) and used for liquid chromatography-mass spectrometry (LC-MS) analysis.

Samples of the final supernatant (5 µL) were automatically injected into the LC-QqQ MS (Triple Quadrupole 6430, Agilent Technologies, Waldbronn, Germany) equipped with an Eclipse Plus C18 (2.1 × 50 mm, 1.8 µm) column and guard column Zorbax SB-C18 (1.8 µm, Agilent) at 26 °C. The mobile phase consisted of 0.02% acetic acid in water (solvent A) and 0.02% acetic acid in acetonitrile (solvent B) at a constant flow rate of 300 µL min^{-1}. A linear gradient was applied as follows: 0–11 min and 5%–60% of B, 11–13 min and 60%–95% of B, 13–17 min and 95% of B, 17–19 min and 95% to 5% of B and 19–20 min and 5% of B. A mass spectrometer ionization source ESI (Electrospray Ionisation) was used with the following conditions: gas temperature of 300 °C, nitrogen flow rate of 10 L min^{-1}, nebulizer pressure of 35 psi and capillary voltage of 4000 V. Analysis of polyamines and phytohormones were performed on Multiple Reaction Monitoring (MRM) of ion pairs to use the following mass transitions: putrescine (Put) (89/72), (B) spermidine (Spd) (203/83), (C) spermine (Spm) (146/72), cytokinin (CK) by zeatin (Zea) (220/136), 1-aminocyclopropane-1-carboxylic acid (ACC) (102/56), abscisic acid (ABA) (263/153), salycilic acid (SA) (137/93), and methyl jasmonate (MeJa) (225/151). Put, Spd, Spm, Zea, and ACC were scanned as positive mode whereas ABA, SA, and MeJa were scanned in the negative mode. Polyamines and phytohormones were quantified via calibration curves using authentic standards (1 to 200 µg and 0.1 to 500 ng, respectively; all of Sigma-Aldrich, St. Louis, Missouri, USA). The data generated were analyzed in *Mass Hunter Workstation* software and results are expressed on a fresh weight (FW) basis.

Enzymatic assays

Superoxide dismutase (SOD), catalase (CAT), peroxidases (POD), and ascorbate peroxidase (APX) were extracted by homogenizing 100 mg of frozen fresh material (third fully expanded leaf from the apex of plants) with 1 mL of the extraction medium (potassium phosphate buffer 0.1 M and pH 6.8; phenylmethylsulfonyl fluoride (PMSF) 1 mM; polyvinylpyrrolidone (PVPP) 1% (w/v); ethylenediaminetetraacetic acid (EDTA) 0.1 mM). The mixture was centrifuged at 10,000 *g* for 15 min, and the supernatant was used as crude enzyme extract. All steps were performed at 4 °C.

SOD activity was determined as described by Del Longo *et al*. (1993). Samples were exposed to 15-W lamps for 5 min before being quantified by absorbance readings at 560 nm. The blank was obtained under the same conditions but in the absence of light. A SOD unit was defined as the enzyme amount required to inhibit 50% of the nitroblue tetrazolium (NBT) photoreduction (Beauchamp and Fridovich, 1971). CAT activity was determined as described by Havir and McHale (1987). The decrease in the absorbance at 240 nm was monitored and the enzymatic activity was calculated using a molar extinction coefficient equal to 36 M^{-1} cm^{-1}. POD activity was determined as described by Kar and Mishra (1976). The increase in the absorbance at 420 nm was monitored and the enzymatic activity was calculated using a molar extinction coefficient equal to 2.47 mM^{-1} cm^{-1} (Chance and Maehley, 1955). APX activity was determined as described by Nakano and Asada (1981). The decrease in the absorbance at 290 nm was monitored and the enzymatic activity was calculated using a molar extinction coefficient equal to 2.8 M^{-1} cm^{-1}. The result of SOD activity was expressed as U min^{-1} mg^{-1} protein, while CAT, POD, and APX were expressed as µmol min^{-1} mg^{-1} protein.

Determination of 20-hydroxyecdysone levels

The preparation of the methanolic extract was performed as described by Corrêa *et al*. (2015). The determination of 20E was done using high-performance liquid chromatography (HPLC) on a device Shimadzu SPD-10Avp (Kyoto, Japan) equipped with ultraviolet (UV) detector set at 245 ηm and column Supelco C18 (30 cm x 7.9 mm diameter) with a slow flow of 0.8 mL min^{-1} and column pressure of 97.6 kgf. The mobile phase consisted of isocratic system with a mixed of HPLC grade methanol and deionized water in the ratio (1:1) (v/v). The volume of the injected sample was 20 µL, running for 15 min. The calibration curve was obtained

by preparing 20E standard solutions (Sigma-Aldrich, St. Louis, MO, USA) in HPLC grade methanol (0 to 120 mg L^{-1}).

RNA extraction, cDNA synthesis, and RT-qPCR analysis

Approximately 100 mg of fresh leaf tissue (third fully expanded leaf from the apex of plants) were ground in liquid nitrogen followed of extraction (total RNA) by TRI Reagent® (Sigma-Aldrich, St. Louis, MO, United States) and treated with DNAse I (Thermo Scientific NanoDrop Technology, Wilmington, DE, USA) to remove genomic DNA contamination. First-strand cDNA was synthesized from 500 ng of the total RNA using the MMLV Reverse Transcriptase (Ludwig Biotec®, Alvorada, RS, Brazil).

Ecdysteroid 25-hydroxylase (*Phantom* - Cyp306a1) and cytochrome P450 family 307 subfamily A (*Spook* - Cyp307a1) expression levels were assessed by qRT-PCR with gene-specific primers. qRT-PCR was conducted on a CFX96 Touch™ (BIO-RAD). The *P. glomerata* glycerol-3-phosphate dehydrogenase gene (*PgGAPDH*) was used as an internal reference gene with specific primers. The primers were obtained from a *P. glomerata* transcriptome (Batista *et al*., 2018). PCR programs were as follow: 2 min at 50 ºC and 10 min at 90 ºC, followed by 40 cycles of 16 s at 95 ºC and 1 min at 60 ºC, and 15 s at 95 ºC, 1 min at 60 ºC, 30 s at 95 ºC, and 15 s at 60 ºC. Transcript levels were determined using the $2^{-\Delta\Delta Ct}$ method (Livak and Schmittgen, 2001) with three biological replicates and at least three technical replicates (reactions).

Statistical analyses

The experiment was designed in a completely randomized design. The data were statistically analyzed by one-way analysis of variance (ANOVA). Gene expression was tested for significant differences using Dunnett's test ($P<0.05$), while all other variables by Tukey's test ($P<0.05$). All of the statistical analyses were performed using the software Genes (Cruz, 2013).

Results

Salt stress inhibits growth

Plants under 120 mM NaCl demonstrated mild symptoms when compared to plants treated with 240, 360 and 480 mM NaCl (Fig. 1). Plants under salt stress showed phenotypic symptoms such as leaf chlorosis and senescence and necrotic spots in the leaf blade (Supplemental Figure S1), particularly at the highest NaCl levels (≥ 240 mM).

Compared to control plants, plant height decreased significantly at 240 (17%), 360 (32%) and 480 (32%) mM NaCl. Decreases were also observed in leaf DW (36 to 57%), stem DW (45 to 73%), and root DW (50 to 78%) (Table 1). Leaf abscission was also significant at 240, 360 and 480 mM treatments (resulting in leaf losses of 0.5, 1.4 and 2.2 g, respectively) as compared with 0 or 120 mM salt treatments (which did not displayed leaf abscission) (Table 1). Taken together, these differences caused decreases in total DW at 240, 360 and 480 mM treatments (40 to 60%) (Table 1).

Salt stress promotes leaf nutritional imbalances

Salt stress induced significant changes in leaf nutritional status. K^+ content increased by 360 and 480 mM (2 times in both), as well as Na^+ increased considerably in 240 to 480 mM NaCl (406–562 times), which led to a high Na^+/K^+ ratio in these treatments (Fig. 2). In parallel, salt stress reduced the levels of P, Mg^{2+}, S, Zn and Mn in 240 to 480 mM NaCl treatments, while the other nutrients (N, Ca^{2+}, Cu and Fe) were not responsive (Fig. 2).

Salt stress negatively affects photosynthetic performance

The *A* decreased significantly by 58, 85 and 99% at 240, 360 and 480 mM NaCl, respectively, relative to the control plants (Fig. 3A). This was accompanied by decreases in g_s, 45, 73 and 95% at 240, 360 and 480 mM of NaCl, respectively (Fig. 3B). *E* responded to salt treatments in a similar way as that of g_s (Fig. 3D). In contrast, C_i significantly increased in plants under 360 and 480 mM of NaCl (13 and 36%, respectively) when compared to the control plants (Fig. 3C).

Compared with controls, there were significant decreases in F_v/F_m (43 and 60% at 360 and 480 mM NaCl, respectively) (Fig. 3E), in qP (32, 51 and 68% at 240,

360 and 480 mM NaCl, respectively) (Fig. 3F), in ETR (49, 76 and 89% at 240, 360 and 480 mM NaCl, respectively) (Fig. 3H), and total chlorophyll content (18, 48, 62 and 57% at 120, 240, 360 and 480 mM NaCl, respectively) (Fig. 3I). In contrast, NQP increased significantly (42, 56 and 78% at 240, 360 and 480 mM NaCl, respectively) (Fig. 3G).

Salt stress strongly affected primary leaf metabolite levels and protein and starch concentrations

Salt stress reduced metabolite levels related to energy reserves (sucrose and starch) and also the protein content at 240, 360 and 480 mM compared to controls (Fig. 4A–C, respectively). In contrast, salt stress increased the levels of metabolites with osmoregulatory roles, such as glucose and fructose whose contents increased at 240, 360 and 480 mM NaCl (Fig. 4D–E), and amino acids which increased significantly at 480 mM compared to controls (Fig. 4F). Notably, there were remarkable increases in proline content (262, 418 and 626% at 240, 360 and 480 mM NaCl, respectively) relative to controls (Fig. 5).

Salt stress induces changes in leaf phytohormone levels

Phytohormone levels varied significantly compared with controls, with increases in ABA (6–9 times in 240 to 480 mM NaCl) (Fig. 6A), ACC (2 times in 360 and 480 mM NaCl) (Fig. 6B), MeJa (2–3 times in 240 to 480 mM NaCl) (Fig. 6C) and SA (33–113 times in 240 to 480 mM NaCl) (Fig. 6D), while Zea showed reductions (68, 70 and 72% at 240, 360 and 480 mM NaCl, respectively) (Fig. 6E). Increases were also observed in Spd (3 times in 360 and 480 mM NaCl) and strongly in Spm (13–19 times in 240 to 480 mM NaCl) (Fig. 6G–H, respectively), which led to a high (Spd+Spm)/Put ratio in all NaCl treatments (11–19 times) (Fig. 6I). Put was unresponsive to the treatments (Fig. 6F).

Salt stress increase activities of antioxidant enzymes

Compared to control plants, their salt-stressed counterparts displayed significant increases in SOD (96, 125 and 106% at 240, 360 and 480 mM, respectively) (Fig. 7A), POD (110, 200 and 259% at 240, 360 and 480 mM, respectively) (Fig. 7C) and APX (32, 40 and 50% at 240, 360 and 480 mM, respectively) (Fig. 7D), while the greatest increases (~150%) in CAT were observed

at 120 and 240 mM NaCl, against 91 and 71% under 360 and 480 mM NaCl, respectively (Fig. 7B).

Mild salt stress increase 20E contents

Whole-plant 20E content increased significantly under 120 mM NaCl (20%) when compared to control treatment, while the other treatments (e.g., 240, 360 and 480 mM NaCl) displayed similar 20E content when compared to control (~5.5 mg g^{-1} DW) (Fig. 8A). In comparison with controls, 20E concentration increased in leaves (47%) but only at 120 mM NaCl (Fig. 8B), but remained unresponsive to salt treatments in the stems (ranging from 0.8 to 1.0 mg g^{-1} DW) (Fig. 8C), whereas in the roots it decreased significantly at 240 (17%), 360 (20%) and 480 (34%) mM NaCl (Fig. 8D).

Salt stress upregulates the Spook *and* Phantom *genes*

The expression of 20E biosynthesis genes was positively influenced by all NaCl concentrations. Compared to controls, *Spook* and *Phantom* were upregulated (4–5 times) under 120 mM NaCl salt stress, but to a lesser extent (3 fold) in the other treatments (240 to 480 mM NaCl) (Fig. 9A–B).

Discussion

To the best of our knowledge, this study is the first to investigate regulation and expression of 20E in response to short-term salt stress. Our data confirmed the hypothesis that salt stress, depending on its severity, enhances 20E production. Mild salt stress (120 mM of NaCl) did not affect photosynthesis, carbohydrate and amino acid pools and ultimately biomass accumulation, but was able to induce higher 20E concentrations and thus higher absolute contents (amounts) of 20E on a per whole-plant basis could be obtained. In contrast, growth was severely affected with increasing stress severity due probably to the impact caused by decreases in photosynthetic performance (and low assimilate availability, e.g., sucrose and starch), which, despite not causing reductions in the concentrations of 20E, led to decreased contents (amounts) of 20E on a per whole-plant basis due to lower plant biomass.

We observed proportionally larger decreases in A than in g_s and ETR, concomitantly with increases in C_i, at concentrations of NaCl ≥ 240 mM. Therefore, impairments to A are unlikely to have been associated with diffusive or photochemical limitations; rather the observed decreases in A were associated with dysfunctions at the level of biochemical reactions to CO_2 fixation. In any case, a range of dysfunctions at the photochemical level were noted under severe salt stress, as inferred from the decreased PSII photochemical efficiency (analyzed as F_v/F_m), which suggests the occurrence of chronic photoinhibition to photosynthesis (Krause and Weis, 1991). Concordant decreases in the fraction of absorbed light that is dissipated photochemically (estimated as q_P) were also noted, suggesting that the stressed plants were likely unable to fully capture and exploit the absorbed energy. In as much as these results were accompanied by lower decreases in ETR than in A, an excess reducing power is expected to be created that can trigger a range of photoinhibitory and photooxidative effects (Maxwell and Johnson, 2000). Here we suggest that the salt-stressed plants cope with such an excess reducing power via heat dissipation, as evidenced by the increased NPQ (Krause and Weis, 1991; Logan et al., 2007). Nevertheless, heat dissipation was proven not to be enough to prevent photoinhibition given the observed decreases in F_v/F_m and other dysfunctions such as leaf chlorosis and abscission. Collectively, imbalances in the photosynthetic apparatus are believed to result in increased ROS production (oxidative stress),

which in turn explain the increased activities of some antioxidant enzymes we analyzed.

In addition to altering their antioxidant system, plants dealt with salt stress by promoting osmotic adjustment (as judged from the increases in sugars such as glucose and fructose, amino acids and proline). These adjustments are consistent with our data of plant water potential, which was unresponsive to the treatments regardless of the osmotic stress that is created by the addition of salts (data not shown). Cytoplasmic osmolytes, besides facilitating water absorption, can also protect and stabilize structures and macromolecules (proteins, membranes, chloroplasts, and lysosomes) (Bohnert *et al*., 1995; Park *et al*., 2016). Such a protective function might be also achieved via the enhanced PA (e.g., spermine and spermidine) levels in salt-stressed plants (Sudhakar *et al*., 2015). Our data additionally suggest an overall hormonal reprogramming due to the stress, e.g., changes in SA, ACC (precursor of ethylene) and CKs which may be involved in signaling to improve salt resistance through osmotic adjustment (Gharbi *et al*., 2017). Increased ACC and decreased Zea can help to explain leaf senescence and abscission (Ghanem *et al*., 2008). Increases in ABA levels can trigger stomata closure, thus helping to decrease water loss (Fahad *et al*., 2015). Finally, the levels of SA, which increased sharply under high NaCl concentrations, can be a strategy for mitigating the negative effects of salt stress (Zheng *et al*., 2018) via counteracting the tradeoffs between growth and defense (Shakirova, 2007; Rivas-San Vicente and Plasencia, 2011). Taken all of the above information together, our data suggest a range of strategies of *P. glomerata* plants to cope with salt stress. Nonetheless, these acclimation responses were proven unsuccessful given that plant growth (coupled with photosynthetic performance and nutritional imbalances) was severely impaired at concentrations equal or above 240 mM NaCl.

All these changes caused by salinity in photosynthetic performance, ion homeostasis and oxidative balance may activate secondary metabolic pathways (Gengmao *et al*., 2015). The current finding of our research is that salt stress upregulated the expression of genes related to 20E biosynthesis pathway, suggesting that abiotic factors may shift the endogenous levels of 20E in plants. In phytosterol (plant sterols) pathways, salt stress enhanced the levels of campesterol, stigmasterol, and *β*-sitosterol in *Avicennia marina* and *Rhizophora stylosa* species, a salt secretor and a non-salt secretor plant, respectively (Basyuni *et al*., 2012). These results

partially corroborate with our data given that phytoecdysteroids biosynthesis is derived from phytosterol synthesis pathway (Tarkowská *et al*., 2016; Moreau *et al*., 2018). Here, possibly, the incipient stress (osmotic stress) and ion toxicity caused by excess salts promoted ROS accumulation which, in turn, may have induced the increase of 20E in *P. glomerata* given that ROS induce the expression of several genes related to the biosynthesis of secondary metabolites (Zhao *et al*., 2005). However, 20E concentration was not further increased with salinity in a concentration-dependent manner, despite the marked overexpression of *Spook* and *Phantom* genes. Likely, severe salt stress was able to dramatically disrupt carbon metabolism (with concomitantly decreased levels of sucrose and starch) and, as a consequence, 20E concentrations were held in check given that the investment in secondary metabolites is linked to carbon availability at the whole-plant scale (Huang *et al*., 2017).

In conclusion, our results show that *P. glomerata* counteracts salt stress via a range of acclimatory strategies (e.g., osmotic adjustment and increased activities of antioxidant enzymes), which might involve an orchestrated reprogramming of hormone levels. However, these strategies were proven unsuccessful given that ion imbalances and depressed photosynthetic performance led to marked decreases in plant growth at NaCl concentrations ≥ 240 mM. Most importantly, mild salt stress (120 mM of NaCl) did not affect photosynthesis and biomass accumulation, and was able to upregulate 20E levels, and thus allowing improved 20E contents in a whole-plant basis. Also, mild salt stress could be used as a strategy to improve 20E production in *P. glomerata*.

References

Abdallah, S.B., Aung, B., Amyot, L., Lalin, I., Lachâal, M., Karray-Bouraoui, N., Hannoufa, A., 2016. Salt stress (NaCl) affects plant growth and branch pathways of carotenoid and flavonoid biosyntheses in *Solanum nigrum*. Acta Physiol. Plant. 38, 72.

Acosta-Motos, J.R., Ortuño, M.F., Bernal-Vicente, A., Diaz-Vivancos, P., Sanchez-Blanco, M.J., Hernandez, J.A., 2017. Plant responses to salt stress: adaptive mechanisms. Agronomy 7, 1–38.

Akula, R., Ravishankar, G.A., 2011. Influence of abiotic stress signals on secondary metabolites in plants. Plant Signal. Behav. 6, 1720–1731.

Almeida, D.M., Oliveira, M.M., Saibo, N.J.M., 2017. Regulation of Na^+ and K^+ homeostasis in plants: towards improved salt stress tolerance in crop plants. Genet. Mol. Biol. 40, 326–345.

Almeida, I.V., Düsman, E., Mattge, G.I., Toledo, F., Reusing, A.F., Vicentini, V.E.P., 2017. *In vivo* antimutagenic activity of the medicinal plants *Pfaffia glomerata* (Brazilian-ginseng) and *Ginkgo biloba*. Genet. Mol. Res. 16(3), gmr16039785.

Alvarez, V.H., Dias, L.E., Ribeiro Jr., E.S., Souza, R.B., Fonseca, C.A., 2001. Métodos de análises de enxofre em solos e plantas. Viçosa: Editora UFV. pp 1–131.

Arora, D., Bhatla, S.C., 2017. Melatonin and nitric oxide regulate sunflower seedling growth under salt stress accompanying differential expression of Cu/Zn SOD and Mn SOD. Free Radic. Biol. Med. 106, 315–328.

Arsovski, A.A., Zemke, J.E., Haagen, B.D., Kim, S.H., Nemhauser, J.L. (2018). Phytochrome B regulates resource allocation in *Brassica rapa*. J. Exp. Bot. 69, 2837-2846.

Assaha, D.V., Ueda, A., Saneoka, H., Al-Yahyai, R., Yaish, M.W., 2017. The role of Na^+ and K^+ transporters in salt stress adaptation in glycophytes. Front. Physiol. 8, 509.

Azevedo-Neto, A.D., Prisco, J.T., Eneas-Filho, J., de-Abreu, C.B., Gomes-Filho, E., 2006. Effect of salt stress on antioxidative enzymes and lipid peroxidation in leaves and roots of high-yielding and low-yielding maize genotypes. Environ. Exp. Bot. 56, 87–94.

Barton, K.E., Boege, K., 2017. Future directions in the ontogeny of plant defence: understanding the evolutionary causes and consequences. Ecol. Lett. 20, 403–411.

Basyuni, M., Baba, S., Kinjo, Y., Oku, H., 2012. Salinity increases the triterpenoid content of a salt secretor and a non-salt secretor mangrove. Aquat. Bot. 97, 17–23.

Bates, L.S., Waldren, R.P., Teare, I.D., 1973. Rapid determination of free proline for water-stress studies. Plant Soil 39, 205–207.

Batista, D.S., Koehler, A.D., Romanel, E., Souza, V.C, Silva, T.D., Almeida, M.C., Maciel, T.E.F., Ferreira, R. P. B., Felipe, S.H.S., Saldanha, C.W., Maldaner, J., Dias, L.L.C., Festucci-Buselli, R.A., Otoni, W.C. *De novo* assembly and transcriptome of *Pfaffia glomerata* uncovers the role of photoautotrophy and the P450 family genes in 20-hydroxyecdysone production. Protoplasma, 1–14.

Beauchamp, C., Fridovich, I., 1971. Superoxide dismutase: improved assays and an assay applicable to acrylamide gels. Anal. Biochem. 44, 276–287.

Bohnert, H.J., Nelson, D.E., Jensen, R.G., 1995. Adaptations to environmental stresses. Plant Cell 7, 1099–1111.

Boo, K.H., Lee, D., Nguyen, Q.V., Jin, S.B., Kang, S., Viet, C.D., Park, S.P., Lee, D-S., Riu, K.Z., 2013. Fluctuation of 20-hydroxyecdysone in individual organs of *Achyranthes japonica* during reproductive growth stage and its accumulation into seed. J. Korean Soc. Appl. Biol. Chem. 56, 335–338.

Chakraborty, K., Bishi, S.K., Goswami, N., Singh, A.L., Zala, P.V., 2016. Differential fine-regulation of enzyme driven ROS detoxification network imparts salt tolerance in contrasting peanut genotypes. Environ. Exp. Bot. 128, 79–90.

Chance, B., Maehly, A.C., 1955. Assay of catalases and peroxidases. Methods Enzymol. 2, 764–817.

Chaves, M.M., Flexas, J., Pinheiro, C., 2009. Photosynthesis under drought and salt stress: regulation mechanisms from whole plant to cell. Ann. Bot. 103, 551–560.

Çiçek, N., Oukarroum, A., Strasser, R.J., Schansker, G., 2017. Salt stress effects on the photosynthetic electron transport chain in two chickpea lines differing in their salt stress tolerance. Photosynth. Res. 136, 291–301.

Corrêa, J.P.O., Vital, C.E., Pinheiro, M.V.M., Batista, D.S., Azevedo, J.F.L., Saldanha, C.W., Cruz, A.C.F., DaMatta, F.M., Otoni, W.C., 2015. *In vitro* photoautotrophic potential and *ex vitro* photosynthetic competence of *Pfaffia glomerata* (Spreng.) Pedersen accessions. Plant Cell Tiss. Organ Cult. 121, 289–300.

Cross, J.M., Von Korff, M., Altmann, T., Bartzetko, L., Sulpice, R., Gibon, Y., Palacios, N., Stitt, M., 2006. Variation of enzyme activities and metabolite levels in 24 *Arabidopsis* accessions growing in carbon-limited conditions. Plant Physiol. 142, 1574–1588.

Cruz, C.D., 2013. GENES - a software package for analysis in experimental statistics and quantitative genetics. Acta Sci. 35, 271–276.

Del Longo, O.T., González, C.A., Pastori, G.M., Trippi, V.S., 1993. Antioxidant defences under hyperoxygenic and hyperosmotic conditions in leaves of two lines of maize with differential sensitivity to drought. Plant Cell Physiol. 34, 1023–1028.

Dias, F.C.R., Martins, A.L.P., Melo, F.C.S.A., Cupertino, M.C., Gomes, M.L.M., Oliveira, J.M., Damasceno, E.M., Silva, J., Otoni, W.C., Matta, S.L.P., 2019. Hydroalcoholic extract of *Pfaffia glomerata* alters the organization of the seminiferous tubules by modulating the oxidative state and the microstructural reorganization of the mice testes. J. Ethnopharmacol. 233, 179–189.

Fahad, S., Hussain, S., Matloob, A., Khan, F. A., Khaliq, A., Saud, S., Hassan, S., Shan, D., Khan, F., Ullah, N., Faiq, M., Khan, M.R., Tareen, A.K., Khan, A., Abid Ullah, A., Nasr Ulla, N., Huang, J., 2015. Phytohormones and plant responses to salinity stress: a review. Plant Growth Regul. 75, 391–404.

FAO and ITPS., 2015. Status of the World's Soil Resources (SWSR) – Main Report. Rome, Italy: Food and Agriculture Organization of the United Nations and Intergovernmental Technical Panel on Soils. pp. 252.

Farhangi-Abriz, S., Torabian, S., 2018. Effect of biochar on growth and ion contents of bean plant under saline condition. Environ. Sci. Poll. Res. 25, 11556–11564.

Fernie, A.R., Roscher, A., Ratcliffe, R.G., Kruger, N.J. 2001. Fructose 2,6-bisphosphate activates pyrophosphate: fructose-6-phosphate 1-phosphotransferase and increases triose phosphate to hexose phosphate cycling in heterotrophic cells. Planta 212, 250–263.

Festucci-Buselli, R.A., Contim, L.A.S., Barbosa, L.C.A., Stuart, J.J., Otoni, W.C., 2008a. Biosynthesis and potential functions of the ecdysteroid 20-hydroxyecdysone – a review. Botany 86, 978–987.

Festucci-Buselli, R.A., Contim, L.A.S., Barbosa, L.C.A., Stuart, J., Otoni, W.C., 2008b. Level and distribution of 20-hydroxyecdysone during *Pfaffia glomerata* development. Braz. J. Plant Physiol. 20, 305–311.

Gengmao, Z., Yu, H., Xing, S., Shihui, L., Quanmei, S., Changhai, W., 2015. Salinity stress increases secondary metabolites and enzyme activity in safflower. Ind. Crops Prod. 64, 175–181.

Ghanem, M.E., Albacete, A., Martínez-Andújar, C., Acosta, M., Romero-Aranda, R., Dodd, I. C., Lutts, S., Pérez-Alfocea, F., 2008. Hormonal changes during salinity-

induced leaf senescence in tomato (*Solanum lycopersicum* L.). J. Exp. Bot. 59, 3039–3050.

Gharbi, E., Martínez, J.P., Benahmed, H., Hichri, I., Dobrev, P.I., Motyka, V., Quinet, M., Lutts, S., 2017. Phytohormone profiling in relation to osmotic adjustment in NaCl-treated plants of the halophyte tomato wild relative species *Solanum chilense* comparatively to the cultivated glycophyte *Solanum lycopersicum*. Plant Sci. 258, 77–89.

Gill, S.S., Tuteja, N., 2010. Reactive oxygen species and antioxidant machinery in abiotic stress tolerance in crop plants. Plant Physiol. Biochem. 48, 909–930.

Hanin, M., Ebel, C., Ngom, M., Laplaze, L., Masmoudi, K., 2016. New insights on plant salt tolerance mechanisms and their potential use for breeding. Front. Plant Sci. 7, 1787.

Havir, E.A., McHale, N.A., 1987. Biochemical and developmental characterization of multiple forms of catalase in tobacco leaves. Plant Physiol. 84, 450–455.

Hossain, M.S., ElSayed, A.I., Moore, M., Dietz, K.J., 2017. Redox and reactive oxygen species network in acclimation for salinity tolerance in sugar beet. J. Exp. Bot. 68, 1283–1298.

Huang, J.B., Reichelt, M., Chowdhury, S., Hammerbacher, A., Hartmann, H., 2017. Increasing carbon availability stimulates growth and secondary metabolites via modulation of phytohormones in winter wheat. J. Exp. Bot. 68, 1251–1263

John, R., Shajitha, P.P., Devassy, A., Mathew, L., 2018. Effect of elicitation and precursor feeding on accumulation of 20-hydroxyecdysone in *Achyranthes aspera* Linn. cell suspension cultures. Physiol. Mol. Biol. Plants 24, 275–284.

Kan, X., Ren, J., Chen, T., Cui, M., Li, C., Zhou, R., Zhang, Y., Liu, H., Deng, D., Yin, Z., 2017. Effects of salinity on photosynthesis in maize probed by prompt fluorescence, delayed fluorescence and P700 signals. Environ. Exp. Bot. 140, 56–64.

Kar, M., Mishra, D., 1976. Catalase, peroxidase, and polyphenoloxidase activities during rice leaf senescence. Plant Physiol. 57, 315–319.

Kaur, H., Bhardwaj, R.D., Grewal, S.K., 2017. Mitigation of salinity-induced oxidative damage in wheat (*Triticum aestivum* L.) seedlings by exogenous application of phenolic acids. Acta Physiol Plant. 39, 221.

Koleška, I., Hasanagić, D., Maksimović, I., Bosančić, B., Kukavica, B., 2017. The role of antioxidative metabolism of tomato leaves in long-term salt-stress response. J. Plant Nut. Soil Sci. 180, 105–112.

Krause, G.H., Weis, E., 1991. Chlorophyll fluorescence and photosynthesis: the basics. Annu. Rev. Plant Biol. 42, 313–349.

Lamhamdi, M., Lafont, R., Rharrabe, K., Sayah, F., Aarab, A., Bakrim, A., 2016. 20-Hydroxyecdysone protects wheat seedlings (*Triticum aestivum* L.) against lead stress. Plant Physiol. Biochem. 98, 64–71.

Li, J.T., Han, X.P., Tang, L., Wang, C., Zhang, W.Y., Ma, J., 2018. 20-Hydroxyecdysone protects wheat seedlings from salt stress. Arch Biol Sci. 70, 379–386.

Maxwell, K., Johnson, G.N., 2000. Chlorophyll fluorescence – a practical guide. J. Exp. Bot. 51, 659–668.

Livak, K.J., Schmittgen, T.D., 2001. Analysis of relative gene expression data using real-time quantitative PCR and the $2^{-\Delta\Delta CT}$ method. Methods 25, 402–408.

Logan, B.A., Adams, W.W., Demmig-Adams, B., 2007. Avoiding common pitfalls of chlorophyll fluorescence analysis under field conditions. Funct. Plant Biol. 34, 853–859.

Maxwell, K., Johnson, G.N., 2000. Chlorophyll fluorescence – A practical guide. J. Exp. Bot. 51, 659–668.

Meloni, D.A., Oliva, M.A., Martinez, C.A., Cambraia, J., 2003. Photosynthesis and activity of superoxide dismutase, peroxidase and glutathione reductase in cotton under salt stress. Environ. Exp. Bot. 49, 69–76.

Miller, G., Suzuki, N., Ciftci-Yilmaz, S., Mittler, R., 2010. Reactive oxygen species homeostasis and signalling during drought and salinity stresses. Plant Cell Environ. 33, 453–467.

Moreau, R.A., Nyström, L., Whitaker, B.D., Winkler-Moser, J.K., Baer, D.J., Gebauer, S.K., Hicks, K.B., 2018. Phytosterols and their derivatives: Structural diversity, distribution, metabolism, analysis, and health-promoting uses. Prog. Lipid Res. 70, 35–61.

Murashige, T., Skoog, F., 1962. A revised medium for rapid growth and bio assays with tobacco tissue cultures. Physiol. Plant. 15, 473–497.

Nakano, Y., Asada, K., 1981. Hydrogen peroxide is scavenged by ascorbate-specific peroxidase in spinach chloroplasts. Plant Cell Physiol. 22, 867–880.

Napoleão, T.A., Soares, G., Vital, C.E., Bastos, C., Castro, R., Loureiro, M.E., Giordano, A., 2017. Methyl jasmonate and salicylic acid are able to modify cell wall

but only salicylic acid alters biomass digestibility in the model grass *Brachypodium distachyon*. Plant Sci. 263, 46–54.

Negrão, S., Schmöckel, S.M., Tester, M., 2017. Evaluating physiological responses of plants to salinity stress. Ann. Bot. 119, 1–11.

Ohyama, K., Suzuki, M., Kikuchi, J., Saito, K., Muranaka, T., 2009. Dual biosynthetic pathways to phytosterol via cycloartenol and lanosterol in *Arabidopsis*. Proc. Natl. Acad. Sci. USA 106, 725–730.

Park, H.J., Kim, W.Y., Yun, D.J., 2016. A new insight of salt stress signaling in plant. Mol. Cells 39, 447–459.

Praxedes, S.C., DaMatta, F.M., Loureiro, M.E., Ferrão, M.A., Cordeiro, A.T. (2006). Effects of long-term soil drought on photosynthesis and carbohydrate metabolism in mature robusta coffee (*Coffea canephora* Pierre var. kouillou) leaves. Environ. Exp. Bot. 56, 263-273.

Reis, S.P., Lima, A.M., Souza, C.R.B., 2012. Recent molecular advances on downstream plant responses to abiotic stress. Int. J. Mol. Sci. 13, 8628–8647.

Richter, J.A., Erban, A., Kopka, J., Zörb, C., 2015. Metabolic contribution to salt stress in two maize hybrids with contrasting resistance. Plant Sci. 233, 107–115.

Rivas-San Vicente, M., Plasencia, J., 2011. Salicylic acid beyond defence: its role in plant growth and development. J. Exp. Bot. 62, 3321–3338.

Sarruge, J.R.S., Haag, H.P., 1974. Análises químicas em plantas. Piracicaba, Brazil: USP-ESALQ. pp.1–56.

Shakirova, F.M., 2007. Role of hormonal system in the manifestation of growth promoting and antistress action of salicylic acid. In: Hayat S., Ahmad A. (Eds) Salicylic acid: A plant hormone. Springer, Dordrecht, pp. 69–89.

Silva, M.L.E., Pereira, A.C., Ferreira, D.S., Esperandim, V.R., Símaro, G.V., Lima, T.C., Januário, A.H., Pauletti, P.M., Rehder, V.L.G., Crevelin, E.J., Cunha, W.R., Crotti, A.E.M., Bastos, J.K., 2017. *In vitro* activities of *Pfaffia glomerata* root extract, its hydrolyzed fractions and pfaffic acid against *Trypanosoma cruzi* Trypomastigotes. Chem. Biodiversity 14, e1600175.

Sudhakar, C., Veeranagamallaiah, G., Nareshkumar, A., Sudhakarbabu, O., Sivakumar, M., Pandurangaiah, M., Kiranmai, K., Lokesh, U., 2015. Polyamine metabolism influences antioxidant defense mechanism in foxtail millet (*Setaria italica* L.) cultivars with different salinity tolerance. Plant Cell Rep. 34, 141–156.

Tarkowská, D., Strnad, M., 2016. Plant ecdysteroids: plant sterols with intriguing distributions, biological effects and relations to plant hormones. Planta. 244, 545–555.

Thussagunpanit, J., Jutamanee, K., Homvisasevongsa, S., Suksamrarn, A., Yamagami, A., Nakano, T., Asami, T., 2017. Characterization of synthetic ecdysteroid analogues as functional mimics of brassinosteroids in plant growth. J. Steroid Biochem. Mol. Biol. 172, 1–8.

Tsukagoshi, Y., Ohyama, K., Seki, H., Akashi, T., Muranaka, T., Suzuki, H., Fujimoto, Y., 2016. Functional characterization of CYP71D443, a cytochrome P450 catalyzing C-22 hydroxylation in the 20-hydroxyecdysone biosynthesis of *Ajuga hairy* roots. Phytochemistry 127, 23–28.

Vardanega, R., Muzio, A.F., Silva, E.K., Prata, A.S., Meireles, M.A.A., 2019. Obtaining functional powder tea from Brazilian-ginseng roots: effects of freeze and spray drying processes on chemical and nutritional quality, morphological and redispersion properties. Food Res. Int. 116, 932–941.

Vighi, I.L., Benitez, L.C., Amaral, M.N., Moraes, G.P., Auler, P.A., Rodrigues, G.S., Deuner, S., Maia, L.C., Braga, E.J.B., 2017. Functional characterization of the antioxidant enzymes in rice plants exposed to salinity stress. Biol. Plant. 61, 540–550.

Wahid, A., Ghazanfar, A., 2006. Possible involvement of some secondary metabolites in salt tolerance of sugarcane. J. Plant Physiol. 163, 723–730.

Wang, Q., Eneji, A.E., Kong, X., Wang, K., Dong, H., 2015. Salt stress effects on secondary metabolites of cotton in relation to gene expression responsible for aphid development. PloS One 10, e0129541.

Wangsawang, T., Chuamnakthong, S., Kohnishi, E., Sripichitt, P., Sreewongchai, T., Ueda, A., 2018. A salinity tolerant japonica cultivar has Na^+ exclusion mechanism at leaf sheaths through the function of a Na^+ transporter OsHKT1; 4 under salinity stress. J. Agron. Crop Sci. 204, 274–284.

Yadav, R.K., Sangwan, R.S., Srivastava, A.K., Sangwan, N.S., 2017. Prolonged exposure to salt stress affects specialized metabolites-artemisinin and essential oil accumulation in *Artemisia annua* L.: metabolic acclimation in preferential favour of enhanced terpenoid accumulation accompanying vegetative to reproductive phase transition. Protoplasma 254, 505–522.

Zhao J., Davis L.C. & Verpoorte R. (2005) Elicitor signal transduction leading to production of plant secondary metabolites. Biotechnol. Adv. 23, 283–333.
Zheng, J., Ma, X., Zhang, X., Hu, Q., Qian, R., 2018. Salicylic acid promotes plant growth and salt-related gene expression in *Dianthus superbus* L. (Caryophyllaceae) grown under different salt stress conditions. Physiol. Mol. Biol. Plants 24, 231–238.

Tables and Figures

Table 1. Growth parameters in fifty-one-day-old *Pfaffia glomerata* plants exposed to different concentrations of NaCl (0 – control, 120, 240, and 480 mM) for 11 consecutive days.

NaCl (mM)	Plant height (cm)	Leaf dry weight (g)	Leaf abscission dry weight (g)	Stem dry weight (g)	Root dry weight (g)	Total dry weight (g)

0	66.0 ±4.9 a	10.3 ±0.4 a	0.0 b	8.6 ±0.4 a	4.4 ±0.3 a	23.2 ±1.0 a
120	65.3 ±7.2 a	8.9 ±0.6 a	0.0 b	8.4 ±0.7 a	4.1 ±0.4 a	21.4 ±1.3 a
240	55.1 ±8.3 b	6. 6 ±0.6 b	0.49 ±0.2 b	4.8 ±0.6 b	2.2 ±0.4 b	14.0 ±1.2 b
360	44.9 ±9.5 c	4.6 ±0.6 b	1.41 ±0.3 a	2.4 ±0.2 c	0.9 ±0.2 c	9.3 ±0.8 c
480	44.8 ±4.1 c	4.4 ±0.6 b	2.17 ±0.3 a	3.2 ±0.1 bc	1.0 ±0.1 bc	10.7 ±0.5 bc

Values represent means ± SE (n = 7). Same letters do not differ at 5% level by Tukey's test.

Figure 1. Fifty-one-day-old *Pfaffia glomerata* plants exposed to different concentrations of NaCl (0 – control, 120, 240, and 480 mM) for 11 consecutive days. Bar = 10 cm.

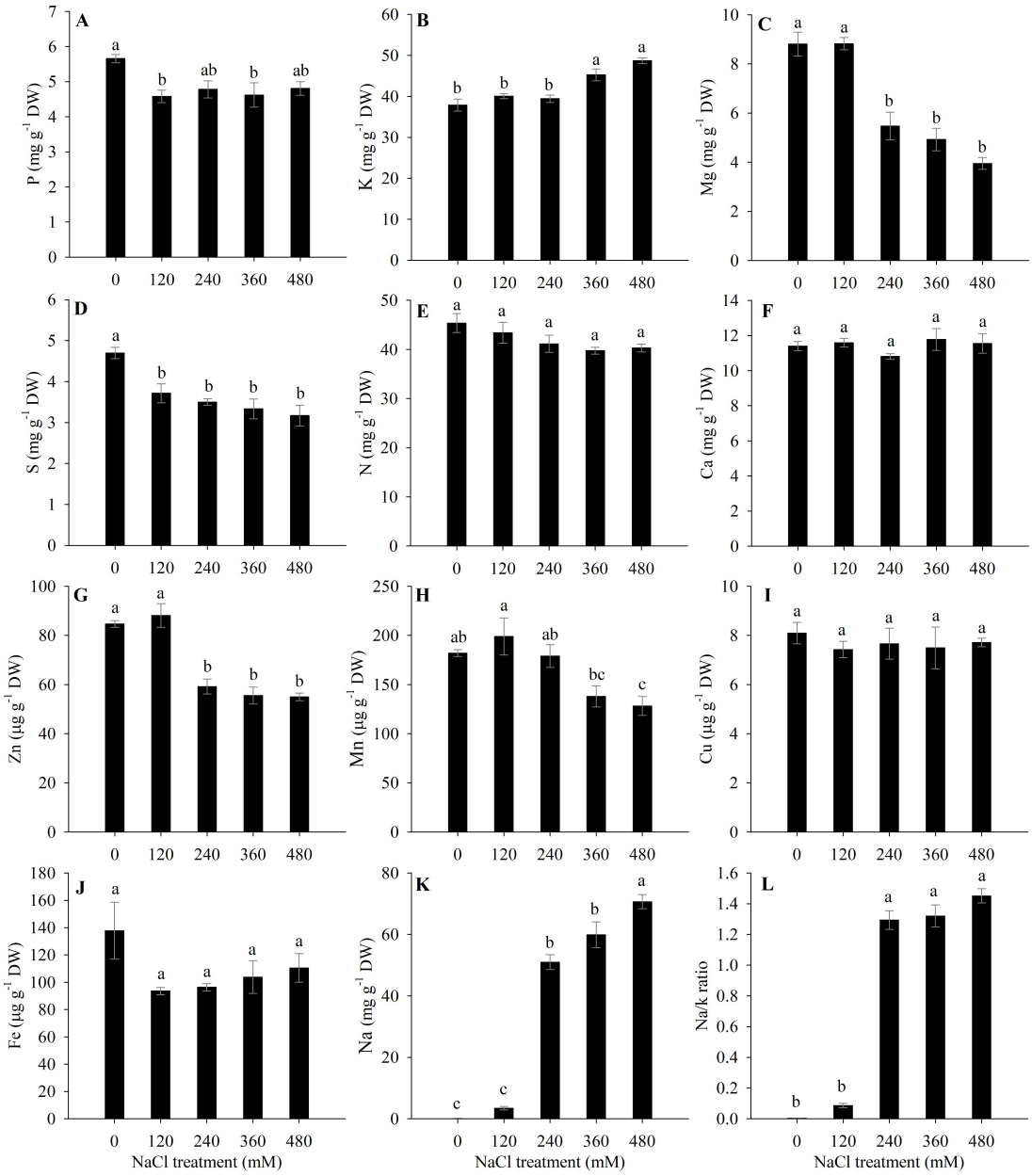

Figure 2. Levels of macronutrient, micronutrient and sodium in fifty-one-day-old *Pfaffia glomerata* plants exposed to different concentrations of NaCl (0 – control, 120, 240, and 480 mM) for 11 consecutive days. A – Phosphorus (P); B – Potassium (K); C – Magnesium (Mg); D – Sulfur (S); E – Nitrogen (N); F – Calcium (Ca); G – Zinc (Zn); H – Manganese (Mn); I – Copper (Cu); J – Iron (Fe); K – Sodium (Na); and L – Na/K ratio. Values represent means ± SE (n=5). Same letters do not differ at 5% level by Tukey's test.

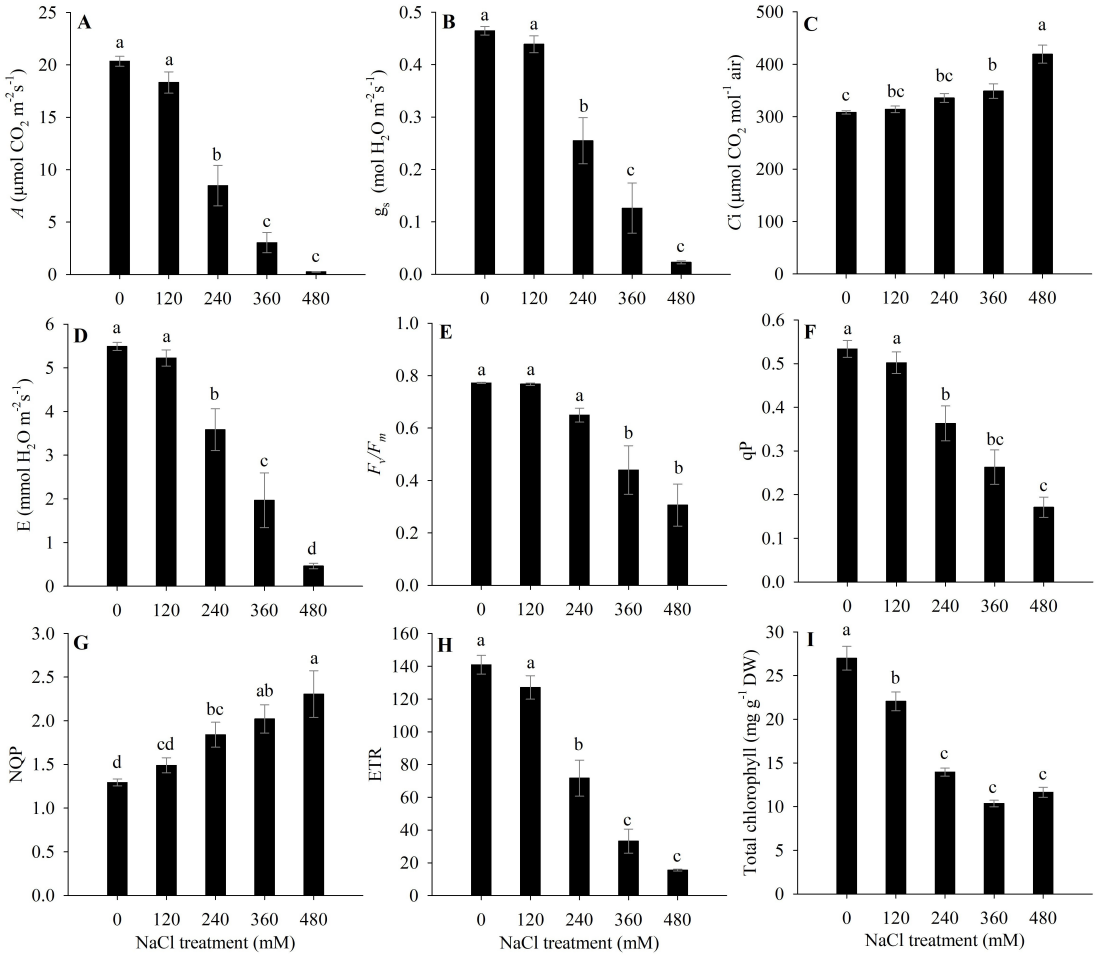

Figure 3. Gas exchange, chlorophyll fluorescence parameters and photosynthetic pigments in fifty-one-day-old *Pfaffia glomerata* plants exposed to different concentrations of NaCl (0 – control, 120, 240, and 480 mM) for 11 consecutive days. A – Net CO_2 assimilation rate (A); B – Stomatal conductance to water vapor (g_s); C – Internal CO_2 concentration (C_i); D – Transpiration rate (E); E – PS II maximum quantum yield (F_v/F_m); F – Photochemical quenching (qP); G – Non-photochemical quenching (NQP); H – Electron transport rate (ETR); and I – Total chlorophyll. Values represent means ± SE (n = 7). Same letters do not differ at 5% level by Tukey's test.

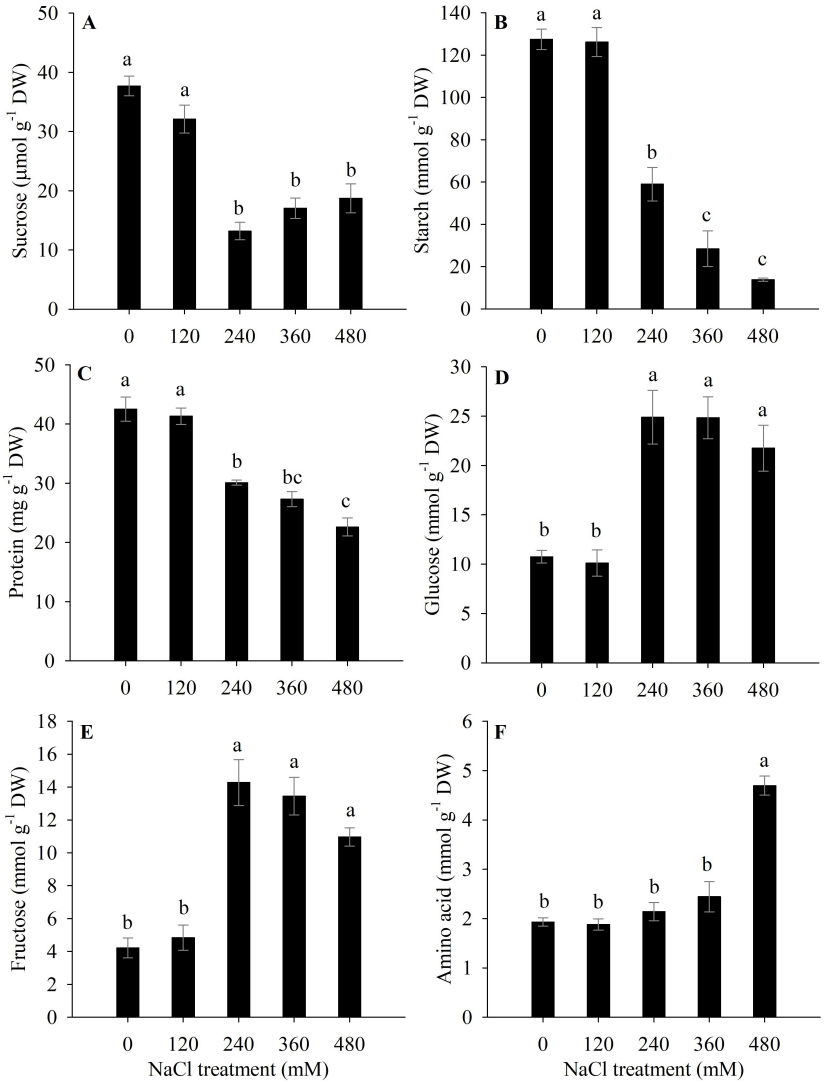

Figure 4. Metabolite levels and protein and starch content in fifty-one-day-old *Pfaffia glomerata* plants exposed to different concentrations of NaCl (0 – control, 120, 240, and 480 mM) for 11 consecutive days. A – Sucrose; B – Starch; C – Protein; D – Glucose; E – Fructose; and F – Amino acid. Values represent means ± SE (n=5). Same letters do not differ at 5% level by Tukey's test.

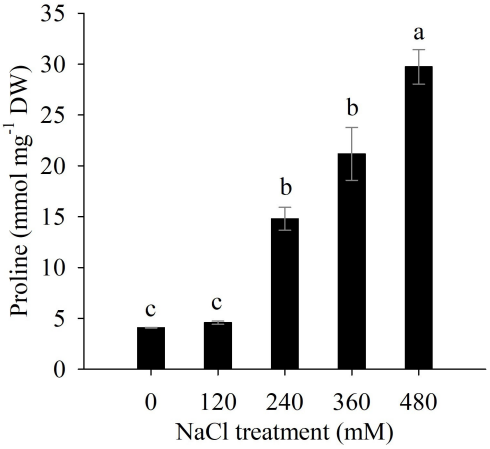

Figure 5. Proline content in fifty-one-day-old *Pfaffia glomerata* plants exposed to different concentrations of NaCl (0 – control, 120, 240, and 480 mM) for 11 consecutive days. Values represent means ± SE (n=4). Same letters do not differ at 5% level by Tukey's test.

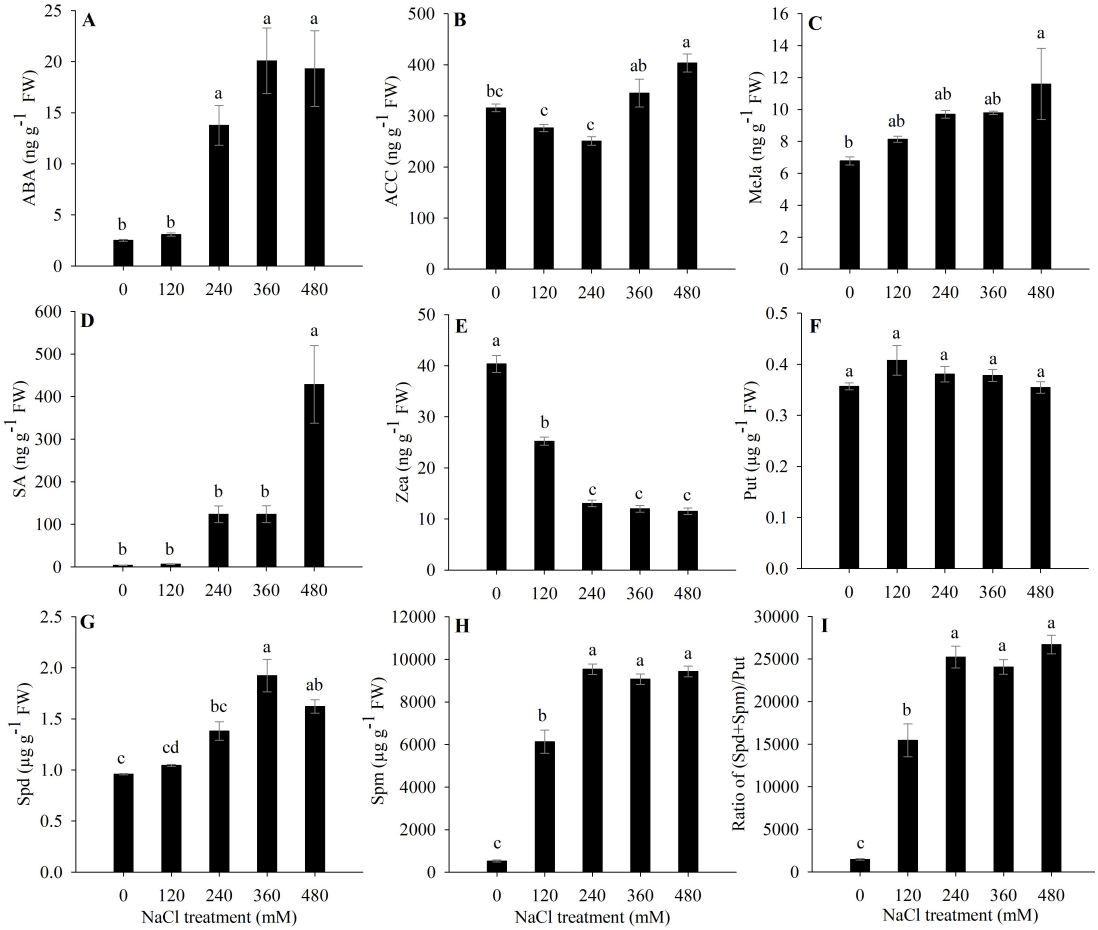

Figure 6. Phytohormone contents in fifty-one-day-old *Pfaffia glomerata* plants exposed to different concentrations of NaCl (0 – control, 120, 240, and 480 mM) for 11 consecutive days. A – Abscisic acid (ABA); B – 1-carboxylic acid-1-aminocyclopropane (ACC); C – Methyl jasmonate (MeJa); D – Salicylic acid (SA); E – Zeatin (Zea), F – Putrescine (Put); G – Spermidine (Spd); H – Spermine (Spm); and I – Ratio of (Spd+Spm)/Put. Values represent means ± SE (n=5). Same letters do not differ at 5% level by Tukey's test.

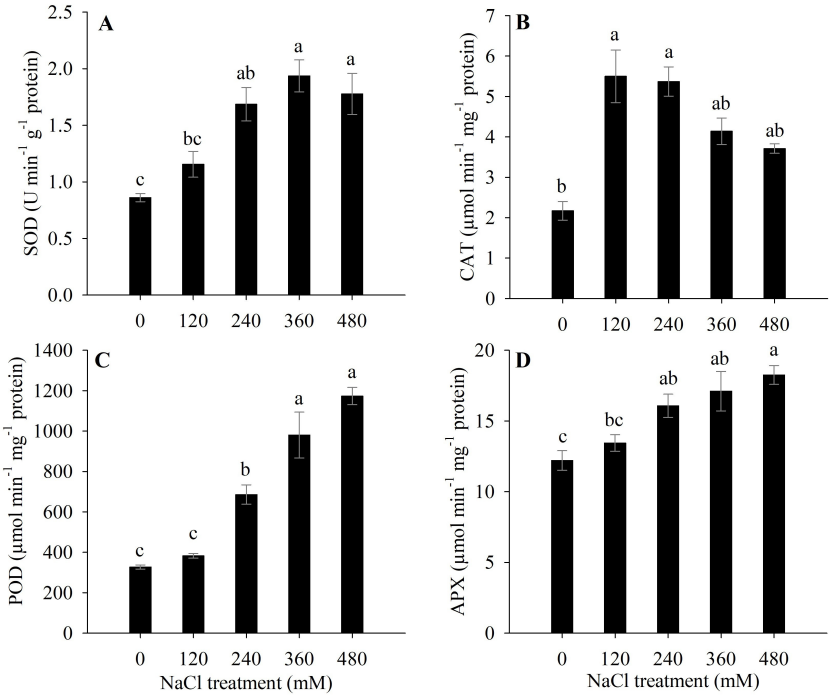

Figure 7. The activities of antioxidant enzymes in fifty-one-day-old *Pfaffia glomerata* plants exposed to different concentrations of NaCl (0 – control, 120, 240, and 480 mM) for 11 consecutive days. A – Superoxide dismutase (SOD); B – Catalase (CAT); C – Peroxidases (POD); and D – Ascorbate peroxidase (APX). Values represent means ± SE (n=4). Same letters do not differ at 5% level by Tukey's test.

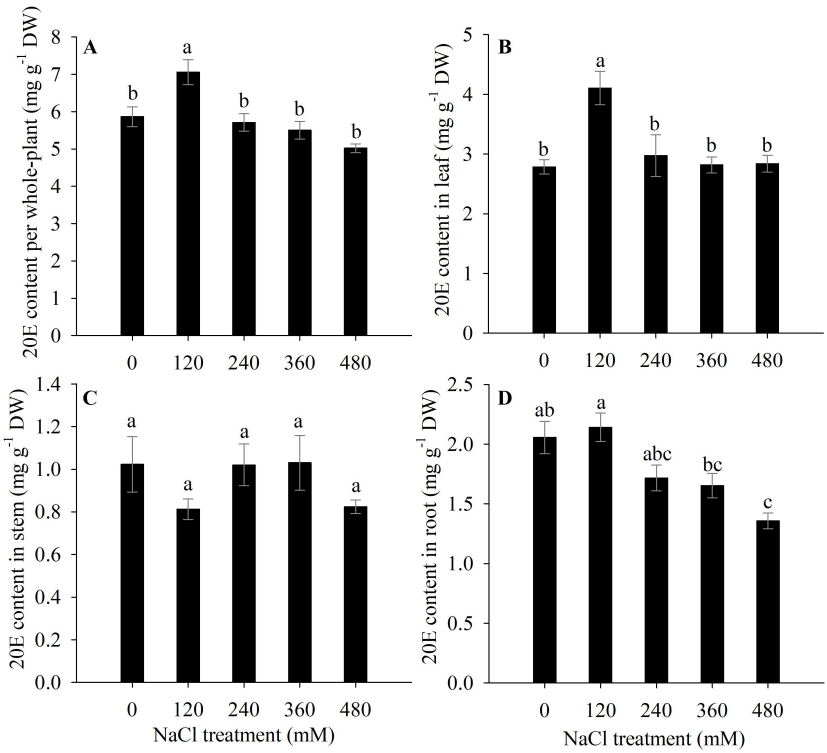

Figure 8. 20-hydroxyecdysone (20E) levels in fifty-one-day-old *Pfaffia glomerata* plants exposed to different concentrations of NaCl (0 – control, 120, 240, and 480 mM) for 11 consecutive days. The content of 20E per: A – plant, B – leaf, C – stem, and D – root. Values represent means ± SE (n = 7). Same letters do not differ at 5% level by Tukey's test.

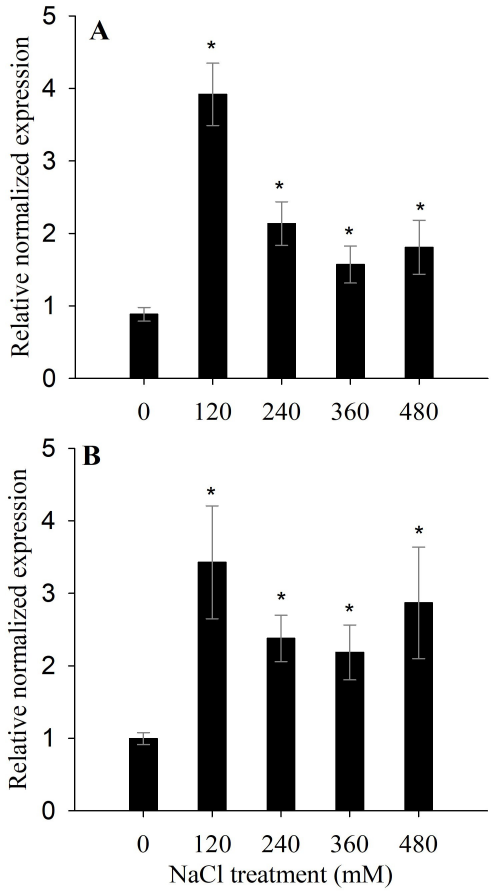

Figure 9. Normalized relative expression of *Phantom* and *Spook* genes in fifty-one-day-old *Pfaffia glomerata* plants exposed to different concentrations of NaCl (0 – control, 120, 240, and 480 mM) for 11 consecutive days. A – *Spook* gene and B – *Phantom* gene. Gene expression relative to the control gene *glyceraldehyde-3-phosphate dehydrogenase*. Values represent means ± SD (n = 4), *$p<0.05$ by Dunnett's test.

Supplemental Figure

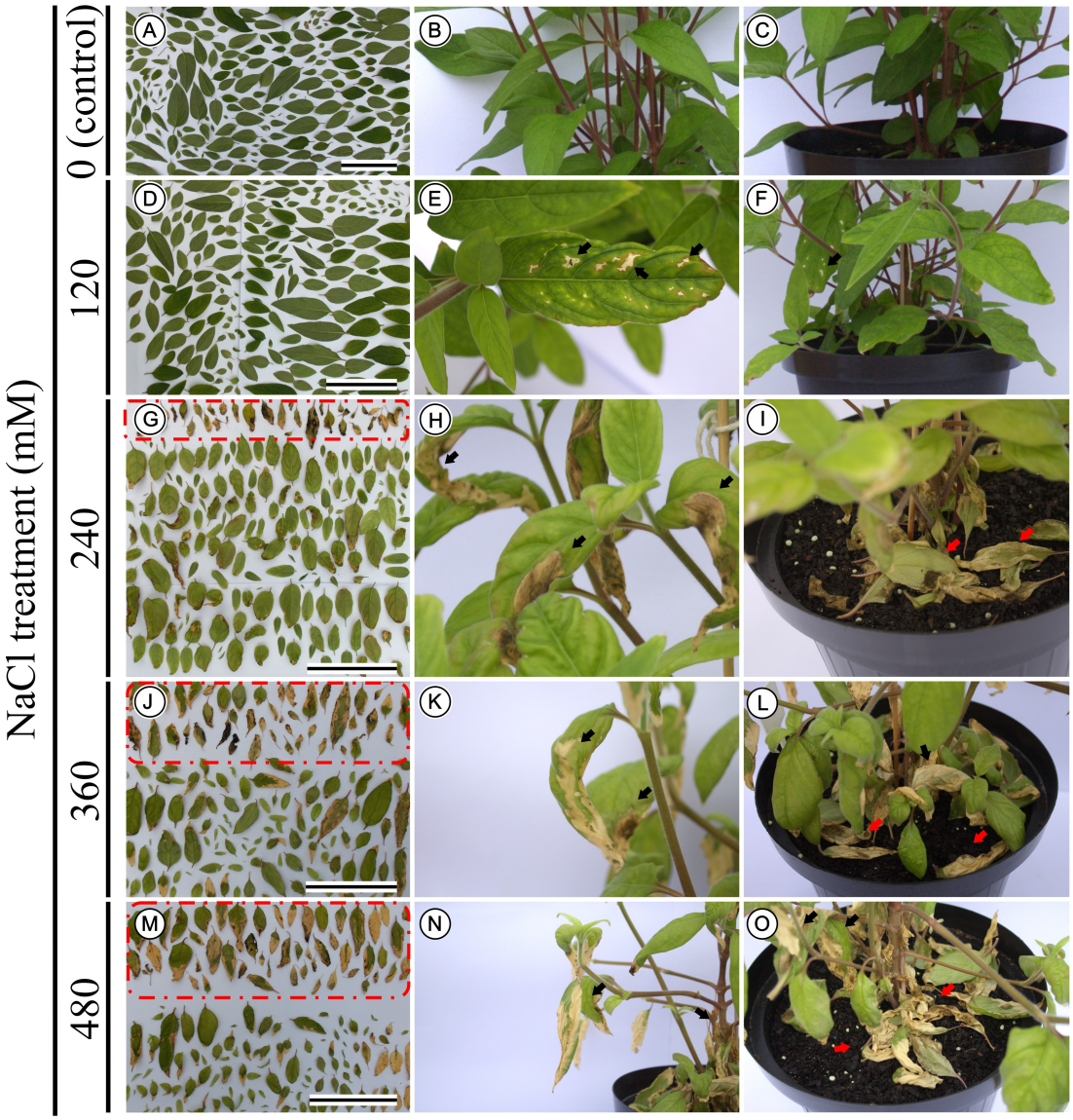

Supplemental Figure S1. The phenotype of fifty-one-day-old *Pfaffia glomerata* plants exposed to different concentrations of NaCl (0 – control, 120, 240, and 480 mM) for 11 consecutive days. Plants under salt stress showed phenotypic symptoms such as leaf chlorosis and senescence and necrotic spots in the leaf blade in a concentration-dependent manner. Dashed lines and red arrows indicate foliar abscission, while black arrow indicates necrosis. Bars = 20 cm.

CHAPTER 2

Accessions of Brazilian-ginseng (*Pfaffia glomerata*) with contrasting anthocyanin content behave differently in growth, antioxidative defense and 20-hydroxyecdysone levels under UV-B radiation

Abstract

Ultraviolet-B (UV-B) radiation is an elicitor of secondary metabolites in plant tissue culture, but the effects on 20-hydroxyecdysone (20E) are still unclear. The 20E may show biotechnological, pharmacological, medical and agrochemical applicability. Here, we use *Pfaffia glomerata*, a medically important species, to understand the impacts of UV-B radiation on their physiological performance, the expression of key genes involved in the 20E biosynthesis and the 20E content. Two accessions (A22 and A43) plants with twenty-day-old grown in *in vitro* were exposed to 0 (control), 2 (6.84 kJ m^{-2}) and 4 (13.84 kJ m^{-2}) h UV-B radiation for 20 consecutive days. Our data showed that UV-B reduced glucose concentration in A22 and A43 under 4 h of exposure (29 and 30%, respectively), while sucrose concentration increased (32 and 57%, respectively). UV-B also differentially impacted the accessions (A22 and A43), where the A22 under 4 h of UV-B reduced total dry weight (8%) and electron transport rate (31%), in contrast, A43 did not changed. Also, only A22 had increased POD activity under 4 h of UV-B (66%), as well as increased gene expression of the 20E pathway and the 20E content under 2 and 4 h of UV-B in leaves (28 and 21%, respectively) and roots (16 and 13%, respectively). This differential performance to UV-B can be explained by the contrasting anthocyanin contents. Notably, A43 displayed 56% more anthocyanin to the former, a possible defense against UV-B. In conclusion, UV-B radiation is a potential elicitor for increasing 20E content in *P. glomerata* grown *in vitro*.

Keywords: abiotic stress, Amaranthaceae, physical elicitor, phytoecdysteroid, ultraviolet-B.

Introduction

Plants have the ability to adapt and respond to complex biotic (e.g., insects, fungi and bacteria) and abiotic (e.g., light, temperature and water availability) interactions to complete their life cycle. Among these factors, light stands out as an energy source for photosynthesis and a regulator of several morphogenetic processes that enable plant growth and development (Lymperopoulos *et al*., 2018). In the photosynthetic process, chlorophyll *a* (Chl *a*; absorbs light at 660 nm and at a lower peak around 400–450 nm) and *b* (Chl *b*; absorbs at 640 and at a lower peak around 425–475 nm) are the main pigments responsible by the capture of light energy in green plants, while carotenoids (carotenes and xanthophylls) also absorb light energy (400–500 nm) for use in photosynthesis, but they act mainly on photoprotection of chlorophyll against photo-damage (Brotosudarmo *et al*., 2018). In addition to the absorption of light in the visible region (400–700 nm), plants perceive light at wavelengths smaller than 400 nm, as exemplified by ultraviolet (UV) radiation (Yang *et al*., 2018).

Despite the stratospheric ozone layer filter out the UV radiation, it is estimated that 8% of this radiation (i.e., UV-A and UV-B) reaches the Earth's surface (Fraikin, 2018). And UV light spectra (UV-A: 320–400 nm, UV-B: 280–320 nm, and UV-C: <280 nm wavelength), which, even if potentially harmful to plants, induce changes on plant secondary metabolism (Schreiner *et al*., 2017; Ghasemi *et al*., 2019). Plants perceive UV-B radiation through a regulatory UV-B photon receptor, UV RESISTANCE LOCUS8 (UVR8), which transforms it into cascades of biochemical signals that result in different morphophysiological responses (Yin and Ulm, 2017; Yang *et al*., 2018).

Overall, UV-B radiation negatively affects photosynthetic performance, reducing CO_2 fixation and O_2 evolution, whilst altering the content of starch and chlorophyll (Dias *et al*., 2018), as also elevated levels of UV-B radiation can induce changes in hormone levels (Vanhaelewyn *et al*., 2016), damage DNA (Ries *et al*., 2000), increase the production of reactive oxygen species (ROS) (Kataria *et al*., 2014) and impair cell cycles (Gómez *et al*., 2018).

The results of injuries caused by UV-B are displayed morphologically in plants, including changes in leaf shape, increased number of lateral branches, less internodes, loss of weight gain and length and leaf area reduction (Cong and Li, 2018). Nevertheless, the phenotype induced by UV-B is diverse, with many apparently contradictory reports on the plant architecture (Robson *et al*., 2015). Thus,

there is a need to develop studies assessing the impact of UV-B on the morphophysiology and secondary metabolism of plant species with agronomic and pharmaceutical interest.

Plants should tolerate, neutralize, or avoid UV-B radiation (Hofmann *et al.* 2003). To cope with UV-B-induced oxidative stress, plants evolved a sophisticated mechanism encompassing filters (Pandey *et al*., 2019), antioxidative defense (Dwivedi *et al*., 2015), production of xanthophyll cycle (Emiliani *et al*., 2018) and secondary metabolites (Zhang *et al*., 2017).

In plant tissue culture, UV-B radiation has been used as an effective strategy to increase secondary metabolites of biotechnological interest, but such changes seem to be diverse enough, as they may positively or negatively affect the increase of metabolites (Schreiner *et al*., 2017), depending on the intensity and time of exposure. Indeed, it is known that UV-B has a strong impact on phenols, flavonoids and anthocyanins, promoting an increase on these compound pathways (Jansen *et al*., 1998; Julkunen-Tiitto *et al*., 2015; Santin *et al*., 2018; Rodríguez-Calzada *et al*., 2019), but the effects on other secondary metabolites (i.e., phytoecdysteroids - PEs) are still unclear.

PEs are steroid hormones analogous to insects (zooecdysteroids - ZEs) found in plants (i.e., 20-hydroxyecdysone - 20E) (Chaubey, 2018). In mammals, they are not biosynthesized, but show medicinal effects (Dinan, 2001; Báthori and Pongracz, 2005; Dinan and Lafont, 2006). 20E molecule is highlighted as one of the most important PEs found in plants (Rharrabe *et al*., 2009), since it has biotechnological, pharmacological, medical and agrochemical potential in the sustainable management of phytophagous insects in agriculture (Festucci-Buselli *et al*., 2008a), and it is produced in relativelylarge amounts in some species, such as in Brazilian-ginseng [*Pfaffia glomerata* (Spreng.) Pedersen] (Amaranthaceae) (Shiobara *et al*., 1993).

P. glomerata stands out among the PEs producing species (i.e., *Spinacia oleracea*, *Chenopodium quinoa*, *Ajuga bracteosa*, and others) due it high levels of 20E accumulation in the roots (Festucci-Buselli *et al*., 2008b, Corrêa *et al*., 2016), which is the main organ marketed in the pharmaceutical industry (Vardanega *et al*., 2017; Han *et al*., 2018; Batista *et al*., 2018). In *in vitro* tissue culture, this species has been studied for the effects of photoautotrophic potential (e.g., Iarema *et al*., 2012; Corrêa *et al*., 2015), CO_2 enrichment (e.g., Saldanha *et al*., 2013; Saldanha *et al*., 2014) and polyploidization (e.g., Gomes *et al*., 2014; Corrêa *et al*., 2016) on 20E

biosynthesis. Likewise, a recent study on *P. glomerata* transcriptome suggested that a P450 family gene (*Phantom*) plays a key role on the 20E biosynthesis route (Batista *et al*., 2018), and it can be targeted in gene expression studies in 20E producing plants under abiotic and biotic elicitors.

It is noteworthy that the main form of *P. glomerata* exploitation is the predatory extraction, contributing in many cases to genetic erosion of this species (Vasconcelos *et al*., 2014). Consequently, the use of plant tissue culture techniques can mitigate these damages by using clonal propagation in large scale, and then perform studies with elicitors aiming to obtain plants with higher 20E levels. Here we describe how the UV-B radiation affects growth, antioxidative defense, 20E content and expression of their biosynthetic genes in two accessions of *in vitro* grown *P. glomerata* plants.

Materials and methods

Plant material and UV-B treatments

Two accessions of *Pfaffia glomerata* (A22 and A43) used in the experiments were taken from the Plant Tissue Culture Laboratory (LCT II, BIOAGRO, Federal University of Viçosa, Brazil) Germplasm Bank. The accession A22 is characterized by the low concentration of anthocyanin in aerial part (i.e., leaf and stem), whereas A43 by the high concentration. These accessions are maintained on a monthly-basis in test tubes (22 mm diameter x 150 mm height) containing 10 mL Murashige and

Skoog (1962) medium supplemented with MS vitamins, 100 mg L^{-1} myo-inositol (Sigma-Aldrich Co, St Louis, MO, USA), 3% sucrose (w/v) and solidified with 5.5 g L^{-1} agar (Phytotechnology Laboratories, LLC, Shawnee Mission, KS, USA), under 25 ± 2 °C, with 36 μmol m^{-2} s^{-1} of irradiance (two fluorescent lamps; 20 W, HO, Osram®, São Paulo, SP, Brazil) and 16-h photoperiod. Herbarium voucher specimens were deposited the Leopoldo Krieger Herbarium-UFJF-Brazil.

A22 and A43 explants with a nodal segment (~1.5 cm) were cultured in glass flasks (6.20 cm diameter x 15.5 mm height and 58 mm of thickness; AZ 200; Embalagens Rio, Nova Friburgo, RJ, Brazil) containing 100 mL Murashige and Skoog (1962) medium supplemented with MS vitamins, 100 mg L^{-1} myo-inositol and 3% sucrose (w/v), pH was adjusted to 5.7 ± 0.1, solidified with 5.5 g L^{-1} agar (Phytotechnology Laboratories, LLC, Shawnee Mission, KS, USA) and sterilized by autoclaving at 121 °C and 1.5 atm for 20 min. The flasks were closed with polypropylene lids with two 10 mm-orifices each covered with 0.45-μm-diameter pore membranes (PTFE; MilliSeal® AVS-045 Air Vent, Tokyo, Japan), which provide a CO_2 exchange rate of 25 μL L^{-1} s^{-1} between the flask and the outside environment (Batista *et al.*, 2017).

The plants were cultivated under 25 ± 2 °C, with 60 μmol m^{-2} s^{-1} of irradiance (two fluorescent lamps; 110 W, HO Sylvania T12) and 16-h photoperiod. Twenty-one-day-old plants of each accession (A22 and A43) were subdivided into three treatments: 0 h (control; 0 kJ m^{-2}); 2 h (6.84 kJ m^{-2}) and; 4 h (13.68 kJ m^{-2}) UV-B radiation for 20 consecutive days (Fig. 1). UV-B was artificially produced by five UV-B linear lamp (emiting ultraviolet rays between 280 and 360 nm with a peak at 305–310 nm; Sankyo Denki G15T8E, Tokyo, Japan). The UV-B irradiance was measured by means of a radiometer/photometer (IL 1400A; International Light Technologies, Peabody, MA, USA).

Plant growth parameters

Plant height was measured. Leaf, stem, and root were also individually oven dried at 50 °C until constant mass and their dry weight (DW) were obtained accordingly.

Chlorophyll fluorescence parameters

Chlorophyll fluorescence measurements were made with a portable pulse-modulated chlorophyll fluorometer (Mini Pam, Heinz Walz GmbH, Effeltrich, Germany). Previously dark-adapted (30 min) leaf tissues were illuminated with a weak modulated laser measuring beam to obtain the initial fluorescence (F_0). Plants were subsequently exposed to light for 30 min under 65 µmol m^{-2} s^{-1} of irradiance, and then the fluorescence parameters of the light-adapted plants were measured. A 1,168 µmol m^{-2} s^{-1} flash of saturating light was used to determine the maximum fluorescence level (F_m). The average of the two steady-state levels of fluorescence was regarded as F_s while the average of the fluorescence levels upon saturating light was regarded as F_m'. The minimal fluorescence level of the light-adapted samples, was calculated as $F_o = F_o/\{[(F_m - F_o)/F_m] + (F_o/F_m')\}$ (Oxborough and Baker, 1997). Then, PS II maximum quantum yield (F_v/F_m) was calculated as $F_v/F_m = (F_m - F_o)/F_m$, photochemical quenching (qP) was calculated as $qP = (F_m' - F_s)/(F_m' - F_o')$ and non-photochemical quenching (NQP) was calculated as $NPQ = (F_m - F_m')/F_m'$ (Baker, 2008). The apparent electron transport rate (ETR) was estimated as $ETR = \Phi_{PSII}*PPFD*f*\alpha$ where f is a factor that accounts for the partitioning of energy between PS II and PSI and is assumed to be 0.5, while α is the leaf absorptance by photosynthetic tissues and is assumed to be 0.84 (Maxwell and Johnson, 2000).

Quantification of soluble sugar, starch, protein, amino acid levels and total chlorophyll

Approximately 15 mg lyophilized of the plant aerial part was used for extraction with ethanol according to Praxedes *et al*. (2006). Photosynthetic pigments were determined as described by Arsovski *et al*. (2018). The concentrations of glucose, fructose, and sucrose were determined as reported by Fernie *et al*. (2001), while the proteins and amino acids were analyzed following Cross *et al*. (2006).

Antioxidant enzyme activities

Superoxide dismutase (SOD), catalase (CAT), peroxidases (POD), and ascorbate peroxidase (APX) were extracted by homogenizing 100 mg of frozen fresh material (aerial part) with 1 mL of the extraction medium (potassium phosphate buffer 0.1 M and pH 6.8; phenylmethylsulfonyl fluoride (PMSF) 1 mM; polyvinylpyrrolidone (PVPP) 1% (w/v); ethylenediaminetetraacetic acid (EDTA) 0.1 mM). The supernatants obtained after centrifugation were directly used for

enzymatic assays and protein concentration determinations (Bradford, 1976). SOD activity was determined as described by Del Longo *et al*. (1993). A SOD unit was defined as the enzyme amount required to inhibit 50% of the nitroblue tetrazolium (NBT) photoreduction (Beauchamp and Fridovich, 1971). CAT activity was determined as described by Havir and McHale (1987). POD activity was determined as described by Kar and Mishra (1976). APX activity was determined as described by Nakano and Asada (1981). The result of SOD activity was expressed as U min^{-1} mg^{-1} protein, while CAT, POD, and APX were expressed as µmol min^{-1} mg^{-1} protein.

Determination of anthocyanin content

Total anthocyanins were determined as described by Neff and Chory (1998). Approximately 100 mg homogenized fresh (in liquid nitrogen) of the plant aerial part were used for extraction within 300 mL of methanol acidified with 1% HCl and incubated for 48 h. Subsequently, 200 µL of distilled water and 500 µL of chloroform were added to the homogenate and centrifuged at 14,000 *g* for 10 min. Total anthocyanins were determined by measuring the A530 and A657 of the aqueous phase and expressed in (A657–A530) per fresh weight (FW).

RNA extraction, cDNA synthesis, and RT-qPCR analysis

Total RNA was isolated of approximately 100 mg of fresh tissue (aerial part) using TRI Reagent® (Sigma-Aldrich, St. Louis, MO, USA) and treated with DNase I (Thermo Scientific NanoDrop Technologies, Wilmington, DE, USA) to remove genomic DNA. First-strand cDNA was synthesized from the total RNA using the Super Script™ III, First-Strand Synthesis System Kit (Invitrogen®, Carlsbad, CA, USA), diluted to a concentration of 10 ng L^{-1}. The genes that participate in the 20-hydroxyecdysone biosynthesis pathway *phantom* and *spook* were obtained from a *P. glomerata* transcriptome (Batista et al. 2018) and the gene *glyceraldehyde-3-phosphate dehydrogenase* was used as internal reference (Batista *et al*., 2019 – *Submitted*). Real-time RT-PCR was performed on a CFX96 Touch™ Real-Time PCR Detection System (BIO-RAD), using qPCR-SYBR-Green mix/Rox (Ludwig Biotec®, Alvorada, RS, Brazil). The qPCR reactions were carried out in duplicate for three biological replicates, in a reaction volume of 10 µL (4 µL SYBR-Green, 1 µL (4 µM) each primer, 2 µL diethylpyrocarbonate-treated water and 1 µL (40 ng) cDNA sample). The amplification conditions were performed using the following steps: 2

min at 50ºC and 10 min at 95ºC, followed by 40 cycles of 95ºC for 16 s and 60ºC for 60 s, and the melting curve performed from 60 to 95°C at 0.1°C/s. The comparative cycle threshold method ($2^{-\Delta\Delta Ct}$) (Livak and Schmittgen, 2001) was applied to calculate the fold-change of the target genes.

Determination of 20-hydroxyecdysone content

The preparation of the methanolic extract was performed as reported by Corrêa *et al*. (2015). 20E determination was done using high-performance liquid chromatography (HPLC) on a device Shimadzu SPD-10Avp (Kyoto, Japan) equipped with ultraviolet (UV) detector set at 245 nm and column Supelco C18 (30 cm x 7.9 mm diameter) with a slow flow of 0.8 mL min^{-1} and column pressure of 97.6 kgf. The mobile phase consisted of HPLC grade methanol and deionized water in the ratio (1:1) (v/v). The volume of the injected sample was 20 µL, running for 15 min. The 20E standard was purchased from Sigma-Aldrich (St. Louis, MO, USA).

Statistical analyzes

The design was completely randomized in a 2 x 3 factorial (two accessions: A22 and A43 and three exposure-times to UV-B radiation: 0, 2 and 4 h) consisting of six replications each treatment. The data were statistically analyzed by one-way analysis of variance (ANOVA), with the means compared by Tukey's test (growth parameters, chlorophyll fluorescence parameters, soluble sugar, starch, protein, amino acid, total chlorophyll, antioxidant enzyme activities, anthocyanin and 20-hydroxyecdysone content) or Dunnet's test (gene expression), with a significance of 5%. All of the statistical analyses were performed using the software Genes (Cruz, 2013).

Results

Growth parameters

UV-B radiation significantly reduced stem dry weight in accessions A22 and A43 under 4 h (17 and 21%, respectively) (Fig. 2C). Both accessions did not display significant differences among treatments in plant height (Fig. 2A), leaf dry weight (Fig. 2B) and root dry weight (Fig. 2D).

In summary, accession A22 displayed higher biomass accumulation compared to accession A43, regardless of the UV-B radiation treatments (control, 2 and 4h UV-B). However, UV-B reduced 8% of total dry weight in accession A22, while accession A43 did not display significant differences (Fig. 2E).

Chlorophyll a *fluorescence parameters and total chlorophyll*

UV-B radiation significantly decreased ETR in accession A22 under 2 and 4 h (35 and 31%, respectively), whereas accession A43 displayed no significant changes (Fig. 3D). The *F*v/*F*m (Fig. 3A), qP (Fig. 3B), NQP (Fig. 3C) and total chlorophyll (Fig. 3E) were not significantly changed by UV-B radiation in both accessions.

Soluble sugar, starch, protein, and amino acid levels

UV-B radiation significantly reduced glucose content in accessions A22 and A43 under 4 h (29 and 30%, respectively) (Fig. 4A), while sucrose content increased

significantly in both accessions under this treatment (32 and 57%, respectively) (Fig. 4C). Fructose content was not affected by UV-B radiation in both accessions (Fig. 4B) and the starch content was significantly reduced only in accession A22 under 4 h (31%) (Fig. 4D).

Amino acid levels increased dependent on the UV-B radiation in both accessions (Fig. 4E), where A22 and A43 increased the amino acid concentration by 46 and 10%, respectively, under 2 h UV-B; and also 87 and 64%, respectively, under 4 h UV-B (Fig. 4E). Protein concentration was not significantly altered in accession A22, while decreased significantly in accession A43 under 2 and 4 h (20 and 17%, respectively) (Fig. 4F).

Activities of antioxidant enzymes

UV-B radiation strongly and significantly affected POD activity only in accession A22 under 4 h by an increase of 66% (Fig. 5A), while CAT showed a significant increase of 34% only in accession A43 access under 2 h UV-B (Fig. 5D). By contrast, both accessions exposed to UV-B radiation did not showed significant changes in SOD and APX activities (Fig. 5B-C).

Anthocyanin accumulation

Accessions A22 and A43 did not displayed changes in anthocyanin levels when exposed to UV-B radiation (Fig. 6). On the other hand, we emphasize that A43 displayed 56% more anthocyanin content as compared to its counterpart (Fig. 6).

Gene expression and 20E content

UV-B radiation significantly influenced *Spook* and *Phantom* expression in A22, while in A43 there were no significant changes (Fig. 7). Accession A22 displayed upregulation of the *Spook* gene under 2 h UV-B (13-fold) (Fig. 7A) and also upregulation of the *Phantom* gene under 2 and 4 h UV-B (5-fold) (Fig. 7B).

The 20E content followed the same pattern of gene expression response (e.g., *Spook* and *Phantom* genes). Under 2 and 4 h UV-B, accession A22 displayed significant increase of 20E in leaves (28 and 21%, respectively) (Fig. 8A) and roots (16 and 13%, respectively) (Fig. 8C), while in the stem there was a reduction of the 20E content in 2h (17%), followed by an increase in 4 h (10%) compared to control

(Fig. 8B). Accession A43 displayed no significant changes between the treatments (~7.5, ~3.8 and ~6.1 mg g^{-1} DW in leaf, stem and root, respectively) (Fig. 8A-C).

Discussion

Physical elicitors (light, osmotic stress, salinity, drought, and thermal stress) have been extensively studied to improve the production of secondary metabolites in plant tissue cultures (Naik and Al–Khayri, 2016). In the present study, we applied UV-B radiation in two accessions of *P. glomerata* grown *in vitro*. Our findings revealed that UV-B radiation differentially impacted on the biomass, physiological features and gene expression and 20E content in the accessions A22 and A43. Although UV-B radiation has the potential to increase the 20E content, this response may be linked to physiological characteristics of this accessions, which may favor (i.e., A22) or hinder (i.e., A43) the 20E pathway.

While UV-B reduced the biomass and ETR in A22, in the A43, did not affect the accumulation of biomass and chlorophyll *a* fluorescence. This suggests that A43 can pursue physiological traits that promote greater tolerance against UV-B. Damages in the photosynthetic machinery directly contribute to the reduction of assimilated biosynthesis, such as the concentration of starch which, in turn, also reduces the biomass in a whole-plant (Hollósy, 2002). An explanation for this is that the amounts of ATP and NADP are reduced, affecting the ability to regenerate ribulose-1,5-bisphosphate (Correia *et al*., 1999). Indeed, UV-B mainly affects photosystem II complex, including the redox-active tyrosines, the Mn cluster, as well as quinone electron acceptors (Q_A and Q_B), causing inactivation of the electron transport chain (reduction of ETR in A22) (Kataria *et al*., 2014). And photosystem II

damage is also attributed to ROS produced as a by-product of electron transport malfunction caused for UV-B (Jansen *et al*., 1998; Tripathi *et al*., 2017).

Given that sugars soluble (glucose, fructose, and sucrose) are altered by UV-B radiation (Yun *et al*., 2018), as observed in this study, where the A22 and A43 displayed reduced glucose concentration and increased sucrose. Changes involving sugar metabolism in plants under stress conditions occur because carbon skeletons are essential for the synthesis of numerous compounds that are involved in anti-oxidative protection (Couée *et al*., 2006; Rosa *et al*., 2009). For example, against UV-B, sucrose biosynthesis by sucrose synthase (SS) and sucrose phosphate synthase (SPS) may be a supply to initiate repair processes in cell membrane systems in affected cells (Barsig *et al*., 1998).

Here, both accessions (A22 and A43) increased the amino acids concentration submitted to UV-B. Overall, amino acids have been reported as acting osmolyte, regulation of ion transport, modulating stomatal opening, and detoxification of heavy metals in plants under stress conditions (Rai, 2002). However, even if amino acids play a crucial role in plant metabolism to mitigate the harmful effects of UV-B oxidative stress (Sergiev *et al*., 2018), maybe the increase in amino acids levels found here is a secondary response to the harmful effect of UV-B in *P. glomerata* and other strategies (i.e., anthocyanins and antioxidant enzymes) may be involved in the combat the damages caused by UV-B.

Interestingly, A43 displays higher anthocyanin concentrations compared to A22, which may explain the higher tolerance of this accession under UV-B. These results are supported by the findings of Kamada (2006), in which they observed a broad phenotypic plasticity in anthocyanin at leaves and stems of 64 *P. glomerata* accessions grown under field conditions. Possibly, the high concentration of anthocyanin mitigates the harmful effects of UV-B, which can lead to damages in the photosynthetic apparatus and, consequently, reduction of biomass in a whole-plant level. It is strongly suggested that anthocyanins act in the prevention of damages caused, directly or indirectly, by UV radiation (photoprotective action) (Gould *et al*., 2018). This photoprotective action of anthocyanins can be subdivided into three main points under the mode of action in plants: (i) sunscreen against excess light; (ii) absorption of UV-B radiation and reduction of its harmful effects, such as photoinhibition and DNA damage; and (iii) mitigation of oxidative damage in leaves by the capture of reactive oxygen species (ROS) (Gould *et al*., 2018).

It is well reported that the antioxidant enzymes in plants are an important defense system to detoxify ROS (Saini *et al*., 2018). POD activity was markedly influenced by UV-B radiation in A22. In plants exposed to UV-B, the increase in POD activity may be linked to building up of stronger walls (Passardi *et al*., 2005), since lignin accumulation increases (Rozema *et al*., 1997). Besides, the increase in enzymes activity related to anti-oxidative system (i.e., POD) suggest that detoxification of ROS is important for the survival of *P. glomerata* plants exposed to UV-B stress. In fact, ROS cause cell damage, but it is known that they can also act on signaling for the production of secondary metabolites in plants (Zhao *et al*., 2005). The lower photoprotection due to the lower anthocyanin concentration may have led to more severe stress in A22 in response to increased ROS (indirectly suggested by the increase in POD activity), and positively regulated *Spook* and *Phantom*, which also led to increased 20E synthesis. Consequently, bearing in mind the wide genetic and morphological variation presented in *P. glomerata* germplasm collection, as initially well-characterized by Kamada *et al*. (2009), the evaluation of different accessions of *P. glomerata* under UV-B radiation is required to discover plants that are highly responsive to UV-B elicitation and that also have phenotypic plasticity to maintain the biomass accumulation at a whole-plant level.

In conclusion, our data show that two *P. glomerata* accessions behave differently under UV-B stress. Likely, anthocyanins play a crucial role against UV-B radiation, modulating the impact on the 20E synthesis in *P. glomerata* grown *in vitro* (Fig. 9). Accession A22 display lower anthocyanin concentration, this facilitates the reduction of ETR, starch content and total dry mass by UV-B stress. To counteract ROS production, A22 mainly increases POD activity. Moreover, ROS also promote orchestrated signaling leading to an upregulation of 20E genes and increasing the 20E content. By contrast to A22, the higher anthocyanin concentration of A43 mitigates the harmful effects of UV-B radiation and, consequently, there is no stress induction sufficient that leading to loss of total dry weight and increased gene expression and content of 20E. Lastly, UV-B radiation has potential to be used as a strategy to induce the 20E production in *P. glomerata* grown *in vitro*.

References

Arsovski AA, Zemke JE, Haagen BD, Kim SH, Nemhauser JL (2018) Phytochrome B regulates resource allocation in *Brassica rapa*. J Exp Bot 69(11):2837–2846.

Baker NR (2008) Chlorophyll fluorescence: a probe of photosynthesis *in vivo*. Annu Rev Plant Biol 59:89–113.

Barsig M, Gehrke C, Schneider K (1998) Effects of UV-B radiation on fine structure, carbohydrates and pigments in *Polytrichum commune*. Bryologist 101:357–365.

Báthori M, Pongrácz Z (2005) Phytoecdysteroids-from isolation to their effects on humans. Curr Med Chem, 12(2):153–172.

Batista DS, Dias LLC, Rêgo MMD, Saldanha CW, Otoni WC (2017) Flask sealing on *in vitro* seed germination and morphogenesis of two types of ornamental pepper explants. Cienc Rural 47(3):e20150245.

Batista DS, Koehler AD, Romanel VC, Souza VC, Silva TD, Almeida MC, Maciel TEF, Bueno PR, Felipe SHS, Saldanha CW, Maldaner J, Carnevalli LL, Festucci-Buselli RA, Otoni WC (2018) *De novo* assembly and transcriptome of *Pfaffia glomerata* uncovers the role of photoautotrophy and the P450 family genes in 20-hydroxyecdysone production. Protoplasma 1–14.

Beauchamp C, Fridovich I (1971) Superoxide dismutase: improved assays and an assay applicable to acrylamide gels. Anal Biochem 44:276–287.

Bradford MM (1976) A rapid and sensitive method for the quantitation of microgram quantities of protein utilizing the principle of protein-dye binding. Anal Biochem 72(1–2): 248–254.

Brotosudarmo THP, Limantara L, Chandra RD (2018) Chloroplast pigments: structure, function, assembly and characterization. In: Ratnadewi D (Ed.). Plant growth and regulation. London:IntechOpen, pp. 43–59.

Chaubey, MK (2018) Role of phytoecdysteroids in insect pest management: a review. J Agron 17(1):1–10.

Cong W, Li X (2018) The importance of short-term ultraviolet-b radiation in biomass and photosynthetic productivity of *Eichhornia Crassipes* (Mart.) Solms. J Plant Growth Regul 37 (3):896–910.

Corrêa JPO, Vital CE, Pinheiro MVM, Batista DS, Azevedo JFL, Saldanha CW, Cruz ACF, DaMatta FM, Otoni WC (2015) *In vitro* photoautotrophic potential and *ex vitro* photosynthetic competence of *Pfaffia glomerata* (Spreng.) Pedersen accessions. Plant Cell Tissue Organ Cult 121(2):289–300.

Corrêa JPO, Vital CE, Pinheiro MVM, Batista DS, Saldanha CW, Cruz ACF, Notini MM, Freitas DMS, DaMatta FM, Otoni WC (2016) Induced polyploidization increases 20-hydroxyecdysone content, *in vitro* photoautotrophic growth, and *ex vitro* biomass accumulation in *Pfaffia glomerata* (Spreng.) Pedersen. In Vitro Cell Dev Biol-Plant 52(1):45–55.

Correia CM, Areal ELV, Torres-Pereira MS, Torres-Pereira JMG (1999) Intraspecific variation in sensitivity to ultraviolet-B radiation in maize grown under field conditions: II. Physiological and biochemical aspects. Field Crops Res 62(2-3):97–105.

Couée I, Sulmon C, Gouesbet G, El Amrani A (2006) Involvement of soluble sugars in reactive oxygen species balance and responses to oxidative stress in plants. J Exp Bot 57(3):449–459.

Cross JM, Von Korff M, Altmann T, Bartzetko L, Sulpice R, Gibon Y, Palacios N, Stitt M (2006) Variation of enzyme activities and metabolite levels in 24 *Arabidopsis* accessions growing in carbon-limited conditions. Plant Physiol 142:1574–1588.

Cruz CD (2013) GENES – a software package for analysis in experimental statistics and quantitative genetics. Acta Sci 35:271–276.

Del Longo OT, González CA, Pastori GM, Trippi VS (1993) Antioxidant defences under hyperoxygenic and hyperosmotic conditions in leaves of two lines of maize with differential sensitivity to drought. Plant Cell Physiol 34: 1023–1028.

Dias MC, Pinto DC, Correia C, Moutinho-Pereira J, Oliveira H, Freitas H, Silva AMS, Santos C (2018) UV-B radiation modulates physiology and lipophilic metabolite profile in *Olea europaea*. J Plant Physiol 222:39–50.

Dinan L (2001) Phytoecdysteroids: biological aspects. Phytochemistry 57(3):325–339.

Dinan L, Lafont R (2006) Effects and applications of arthropod steroid hormones (ecdysteroids) in mammals. J Endocrinol 191(1):1–8.

Dwivedi R, Singh VP, Kumar J, Prasad SM (2015) Differential physiological and biochemical responses of two *Vigna* species under enhanced UV-B radiation. J Radiat Res Appl Sci 8(2):173–181.

Emiliani J, D'Andrea L, Ferreyra MLF, Maulión E, Rodriguez E, Rodriguez-Concepción M, Casati, P (2018) A role for *β*, *β*-xanthophylls in *Arabidopsis* UV-B photoprotection. J Exp Bot 69(20), 4921–4933.

Fernie AR, Roscher A, Ratcliffe RG, Kruger NJ (2001) Fructose 2,6-bisphosphate activates pyrophosphate: fructose-6-phosphate 1-phosphotransferase and increases triose phosphate to hexose phosphate cycling in heterotrophic cells. Planta 212(2):250–263.

Festucci-Buselli RA, Contim LA, Barbosa LCA, Stuart J, Otoni WC (2008a) Biosynthesis and potential functions of the ecdysteroid 20-hydroxyecdysone—a review. Botany 86(9):978–987.

Festucci-Buselli RA, Contim LA, Barbosa LCA, Stuart JJ, Vieira RF, Otoni WC (2008b) Level and distribution of 20-hydroxyecdysone during *Pfaffia glomerata* development. Braz J Plant Physiol 20(4):305–311.

Fraikin GY (2018) Signaling mechanisms regulating diverse plant cell responses to UVB radiation. Biochemistry (Moscow) 83(7):787–794.

Ghasemi S, Kumleh HH, Kordrostami M (2019) Changes in the expression of some genes involved in the biosynthesis of secondary metabolites in *Cuminum cyminum* L. under UV stress. Protoplasma 256:279–290.

Gomes SSL, Saldanha CW, Neves CS, Trevizani M, Raposo NRB, Notini MM, Santos MO, Campos JMS, Otoni WC, Viccini LF (2014) Karyotype, genome size, and *in vitro* chromosome doubling of *Pfaffia glomerata* (Spreng.) Pedersen. Plant Cell Tissue Organ Cult 118(1):45–56.

Gómez MS, Falcone Ferreyra ML, Sheridan ML, Casati P (2018) Arabidopsis E2Fc is required for the DNA damage response under UV-B radiation epistatically over the microRNA396 and independently of E2Fe. Plant J Online First. https://doi.org/10.1111/tpj.14158

Gould KS, Jay-Allemand C, Logan BA, Baissac Y, Bidel LP (2018) When are foliar anthocyanins useful to plants? Re-evaluation of the photoprotection hypothesis using *Arabidopsis thaliana* mutants that differ in anthocyanin accumulation. Environ Exp Bot 154:11–24.

Han YZ, Zhou Y, Zhang ZT, Niu SY, Liu XH, Jia XY (2018) Three new noroleanane-type triterpenes from the roots of *Pfaffia glomerata*. J Asian Nat Prod Res 20(5):460–466.

Havir EA, McHale NA (1987) Biochemical and developmental characterization of multiple forms of catalase in tobacco leaves. Plant Physiol 84:450–455.

Hofmann RW, Campbell BD, Bloor SJ, Swinny EE, Markham KR, Ryan KG, Fountain DW (2003) Responses to UV-B radiation in *Trifolium repens* L. – physiological links to plant productivity and water availability. Plant Cell Environ 26:603–612.

Hollósy F (2002) Effects of ultraviolet radiation on plant cells. Micron 33(2):179–197.

Iarema L, Cruz ACF, Saldanha CW, Dias LLC, Vieira RF, Oliveira EJ, Otoni WC (2012) Photoautotrophic propagation of Brazilian ginseng [*Pfaffia glomerata* (Spreng.) Pedersen]. Plant Cell Tissue Organ Cult 110(2):227–238.

Jansen MA, Gaba V, Greenberg BM (1998) Higher plants and UV-B radiation: balancing damage, repair and acclimation. Trends Plant Sci 3(4):131–135.

Julkunen-Tiitto R, Nenadis N, Neugart S, Robson M, Agati G, Vepsäläinen J, Zipoli G, Nybakken L, Winkler B, Jansen MA (2015) Assessing the response of plant flavonoids to UV radiation: an overview of appropriate techniques. Phytochem Rev 14(2):273–297.

Kamada T (2006) Avaliação da diversidade genética de populações de fáfia (*Pfaffia glomerata* (Spreng.) Pedersen) por RAPD, caracteres morfológicos e teor de beta-ecdisona. Tese de doutorado, Universidade Federal de Viçosa, Viçosa, MG, Brazil. Available in: http://locus.ufv.br/handle/123456789/1298

Kamada T, Picoli EAT, Vieira RF, Barbosa LCA, Cruz CD, Otoni WC (2009) Variação de caracteres morfológicos e fisiológicos de populações naturais de *Pfaffia glomerata* (Spreng.) Pedersen e correlação com a produção de β-ecdisona. Rev Bras Pl Med 11(3): 247–256.

Kar M, Mishra D (1976) Catalase, peroxidase, and polyphenoloxidase activities during rice leaf senescence. Plant Physiol 57:315–319.

Kataria S, Jajoo A, Guruprasad KN (2014) Impact of increasing ultraviolet-b (UV-B) radiation on photosynthetic processes. J Photochem Photobiol B 137:55–66.

Livak KJ, Schmittgen TD (2001) Analysis of relative gene expression data using real-time quantitative PCR and the $2^{-\Delta\Delta CT}$ method. Methods 25:402–408.

Lymperopoulos P, Msanne J and Rabara R (2018) Phytochrome and phytohormones: working in tandem for plant growth and development. Front Plant Sci 9:1037.

Maxwell K, Johnson GN (2000) Chlorophyll fluorescence – a practical guide. J Exp Bot 51(345):659–668.

Murashige T, Skoog F (1962) A revised medium for rapid growth and bio assays with tobacco tissue cultures. Physiol Plant 15:473–497.

Naik PM, Al–Khayri JM. 2016. Abiotic and biotic elicitors-role in secondary metabolites production through *in vitro* culture of medicinal plants. In: Shanker AK, Shanker C (Ed.). Abiotic and biotic stress in plants – recent advances and future perspectives. Rijeka: InTech, pp. 247–277.

Nakano Y, Asada K (1981) Hydrogen peroxide is scavenged by ascorbate-specific peroxidase in spinach chloroplasts. Plant Cell Physiol 22:867–880.

Neff MM, Chory J (1998) Genetic interactions between phytochrome A, phytochrome B, and cryptochrome 1 during *Arabidopsis* development. Plant Physiol 118(1):27–35.

Oxborough K, Baker NR (1997) Resolving chlorophyll a fluorescence images of photosynthetic efficiency into photochemical and non-photochemical components —calculation of qP and Fv′/Fm′ without measuring Fo′. Photosynth Res 54:135–142.

Pandey N, Goswami N, Tripathi D, Rai KK, Rai SK, Singh S, Pandey-Rai S (2019) Epigenetic control of UV-B-induced flavonoid accumulation in *Artemisia annua* L. Planta 249:497–514.

Passardi F, Cosio C, Penel C, Dunand C (2005) Peroxidases have more functions than a Swiss army knife. Plant Cell Rep 24(5):255–265.

Praxedes SC, DaMatta FM, Loureiro ME, Ferrão MA, Cordeiro AT (2006) Effects of long-term soil drought on photosynthesis and carbohydrate metabolism in mature robusta coffee (*Coffea canephora* Pierre var. kouillou) leaves. Environ Exp Bot 56(3):263–273.

Rai VK (2002) Role of amino acids in plant responses to stresses. Biol Plant 45(4):481–487.

Rharrabe K, Bouayad N, Sayah F (2009) Effects of ingested 20-hydroxyecdysone on development and midgut epithelial cells of *Plodia interpunctella* (Lepidoptera, Pyralidae). Pestic Biochem Physiol 93(3):112–119.

Ries G, Heller W, Puchta H, Sandermann H, Seidlitz HK, Hohn B (2000) Elevated UV-B radiation reduces genome stability in plants. Nature 406:98–101.

Robson TM, Klem K, Urban O, Jansen MA (2015) Re-interpreting plant morphological responses to UV-B radiation. Plant Cell Environ 38(5):856–866.

Rodríguez-Calzada T, Qian M, Strid Å, Neugart S, Schreiner M, Torres-Pacheco I, Guevara-González RG (2019) Effect of UV-B radiation on morphology, phenolic compound production, gene expression, and subsequent drought stress responses in chili pepper (*Capsicum annuum* L.). Plant Physiol Biochem 134:94–102.

Rosa M, Prado C, Podazza G, Interdonato R, González JA, Hilal M, Prado FE (2009) Soluble sugars–metabolism, sensing and abiotic stress: a complex network in the life of plants. Plant Signal Behav 4(5):388–393.

Rozema J, Van de Staaij J, Björn LO, Caldwell M (1997) UV-B as an environmental factor in plant life: stress and regulation. Trends Ecol Evol 12(1):22–28.

Saini P, Gani M, Kaur JJ, Godara LC, Singh C, Chauhan SS, Francies RM, Bhardwaj A, Kumar NB, Ghosh MK (2018) Reactive Oxygen Species (ROS): a way to stress survival in plants. In: Zargar S, Zargar M (Ed.) Abiotic stress-mediated sensing and signaling in plants: an omics perspective. Singapore: Springer, pp. 127–153.

Saldanha CW, Otoni CG, Notini MM, Kuki KN, Cruz ACF, Neto AR, Dias LLC, Otoni WC (2013) A CO_2-enriched atmosphere improves *in vitro* growth of Brazilian ginseng [*Pfaffia glomerata* (Spreng.) Pedersen]. In Vitro Cell Dev Biol-Plant 49(4):433–444.

Saldanha CW, Otoni CG, Rocha DI, Cavatte PC, Detmann KDSC, Tanaka FAO, Dias LLC, DaMatta FM, Otoni WC (2014) CO_2-enriched atmosphere and supporting material impact the growth, morphophysiology and ultrastructure of *in vitro* Brazilian-ginseng [*Pfaffia glomerata* (Spreng.) Pedersen] plantlets. Plant Cell Tissue Organ Cult 118(1):87–99.

Santin M, Neugart S, Castagna A, Barilari M, Sarrocco S, Vannacci G, Schreiner M, Ranieri A (2018) UV-B pre-treatment alters phenolics response to *Monilinia*

fructicola infection in a structure-dependent way in peach skin. Front Plant Sci 9:1598.

Schreiner M, Wiesner-Reinhold M, Baldermann S, Hanschen FS, Neugart S (2017) UV-B-induced changes in secondary plant metabolites. In Jordan, BR (Eds.). UV-B radiation and plant life: molecular biology to ecology. Oxfordshire, UK: CABI, pp. 39–57.

Sergiev I, Todorova D, Katerova Z, Brambilla I, Mapelli S, Simova S (2018) Polyamines and amino acids in triticale plants grown on humic acids enriched nutrient solution and treated with UV-B irradiation. Theor Exp Plant Physiol 30(2):153–163.

Shiobara Y, Inoue S, Kato K, Nishiguchi Y, Oishi Y, Nishimoto N, Oliveira F, Akisue G, Akisue MK, Hashimoto G (1993) A nortriterpenoid, triterpenoids and ecdysteroids from *Pfaffia glomerata*. Phytochemistry 32(6):1527–1530.

Tripathi DK, Singh S, Singh VP, Prasad SM, Dubey NK, Chauhan DK (2017) Silicon nanoparticles more effectively alleviated UV-B stress than silicon in wheat (*Triticum aestivum*) seedlings. Plant Physiol Biochem 110:70–81.

Vanhaelewyn L, Prinsen E, Van Der Straeten D, Vandenbussche F (2016) Hormone-controlled UV-B responses in plants. J Exp Bot 67(15):4469–4482.

Vardanega R, Carvalho PI, Albarelli JQ, Santos DT, Meireles MAA (2017) Techno-economic evaluation of obtaining Brazilian ginseng extracts in potential production scenarios. Food Bioprod Process 101:45–55.

Vasconcelos JM, Saldanha CW, Dias LLC, Maldaner J, Rêgo MM, Silva LC, Otoni WC (2014) *In vitro* propagation of Brazilian ginseng [*Pfaffia glomerata* (Spreng.) Pedersen] as affected by carbon sources. In Vitro Cell Dev Biol-Plant 50(6):746–751.

Yang Y, Yang X, Jang Z, Chen Z, Ruo X, Jin W, Wu Y, Shi X, Xu M (2018) UV RESISTANCE LOCUS 8 from *Chrysanthemum morifolium* Ramat (CmUVR8) plays important roles in UV-B signal transduction and UV-B-induced accumulation of flavonoids. Front Plant Sci 9:955.

Yin R, Ulm R (2017) How plants cope with UV-B: from perception to response. Curr Opin Plant Biol 37:42–48.

Yun H, Lim S, Kim YX, Lee Y, Lee S, Lee D, Park K, Sung J (2018) Diurnal changes in CN metabolism and response of rice seedlings to UV-B radiation. J Plant Physiol 228:66–74.

Zhang XR, Chen YH, Guo QS, Wang WM, Liu L, Fan J, Cao Li-Ping, Li C (2017) Short-term UV-B radiation effects on morphology, physiological traits and accumulation of bioactive compounds in *Prunella vulgaris* L. J Plant Interact 12(1):348–354.

Zhao J, Davis LC, Verpoorte R (2005) Elicitor signal transduction leading to production of plant secondary metabolites. Biotechnol Adv 23(4):283–333.

Figures

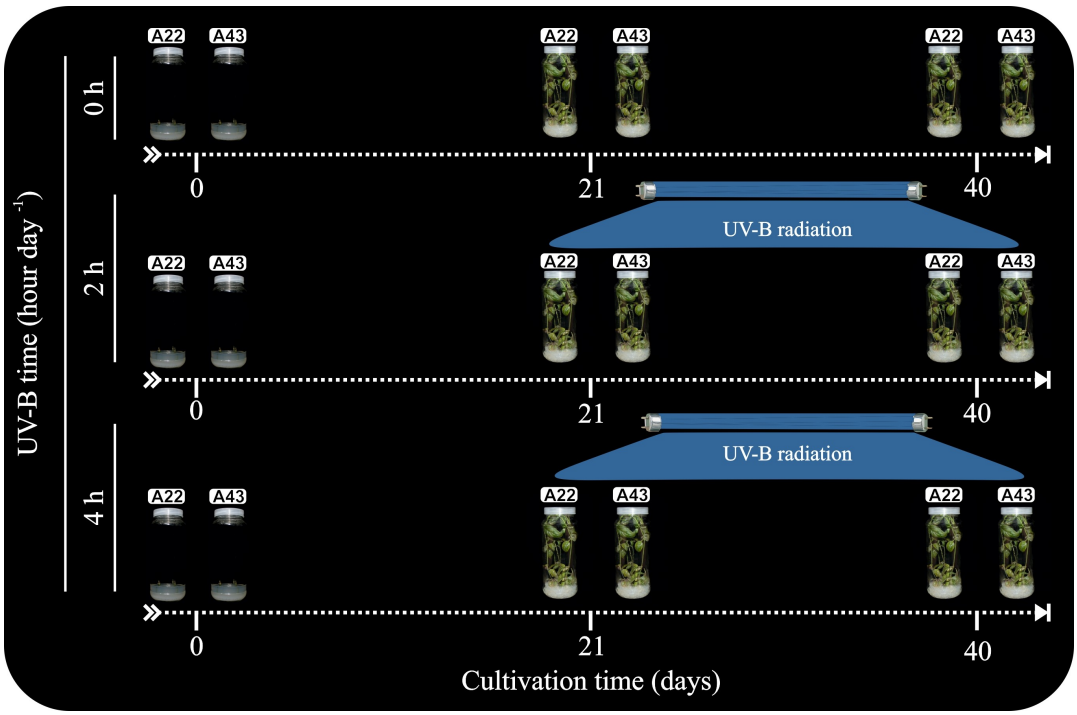

Figure 1. Schematic representation of the experiment design: 0, 2 and 4 h UV-B radiation on *Pfaffia glomerata* grown *in vitro*. Plants were initially cultured for 20 days and then UV-B treatments were applied, which lasted for more 20 days. See further details in “Materials and methods”.

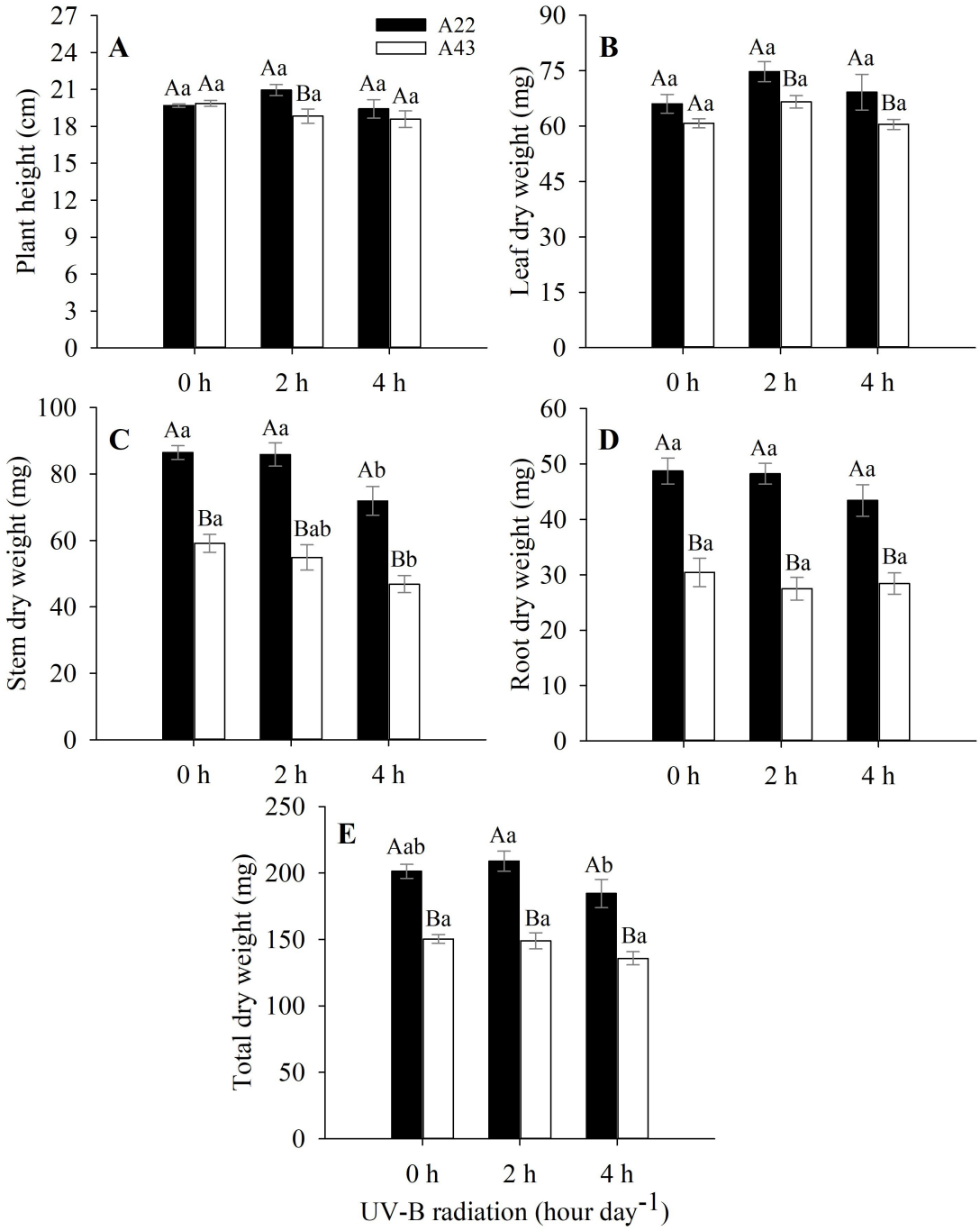

Figure 2. Growth parameters in two *P. glomerata* accessions (A22 and A43) grown *in vitro* under different times of UV-B radiations: 0, 2 and 4 h. **A** – Plant height; **B** – Leaf dry weight; **C** – Stem dry weight; **D** – Root dry weight; and **E** – Total dry weight. Uppercase compares the two accessions at the same time and lowercase compares the same accession at different exposure times. The same uppercase or lowercase letters do not differ at 5% Tukey's test. The bars represent the standard error (n = 6).

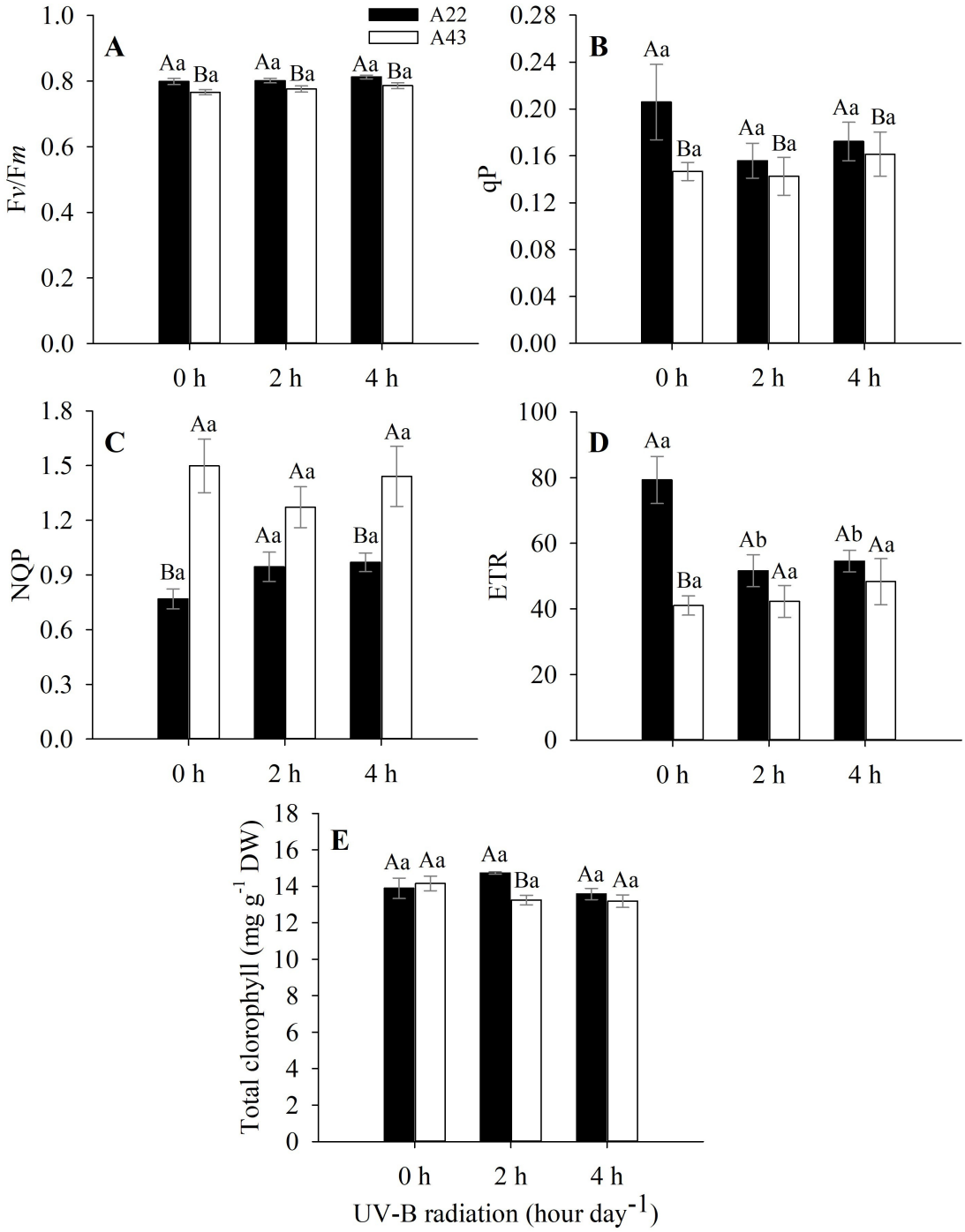

Figure 3. Chlorophyll fluorescence parameters and photosynthetic pigments in two *P. glomerata* accessions (A22 and A43) grown *in vitro* under different times of UV-B radiations: 0, 2 and 4 h. **A** – PS II maximum quantum yield (*F*v/*F*m); **B** – Photochemical quenching (qP); **C** – Non-photochemical quenching (NQP); **D** – Electron transport rate (ETR); and **E** – Total chlorophyll. Uppercase compares the two accessions at the same time and lowercase compares the same accession at different exposure times. The same uppercase or lowercase letters do not differ at 5% Tukey's test. The bars represent the standard error n = 4).

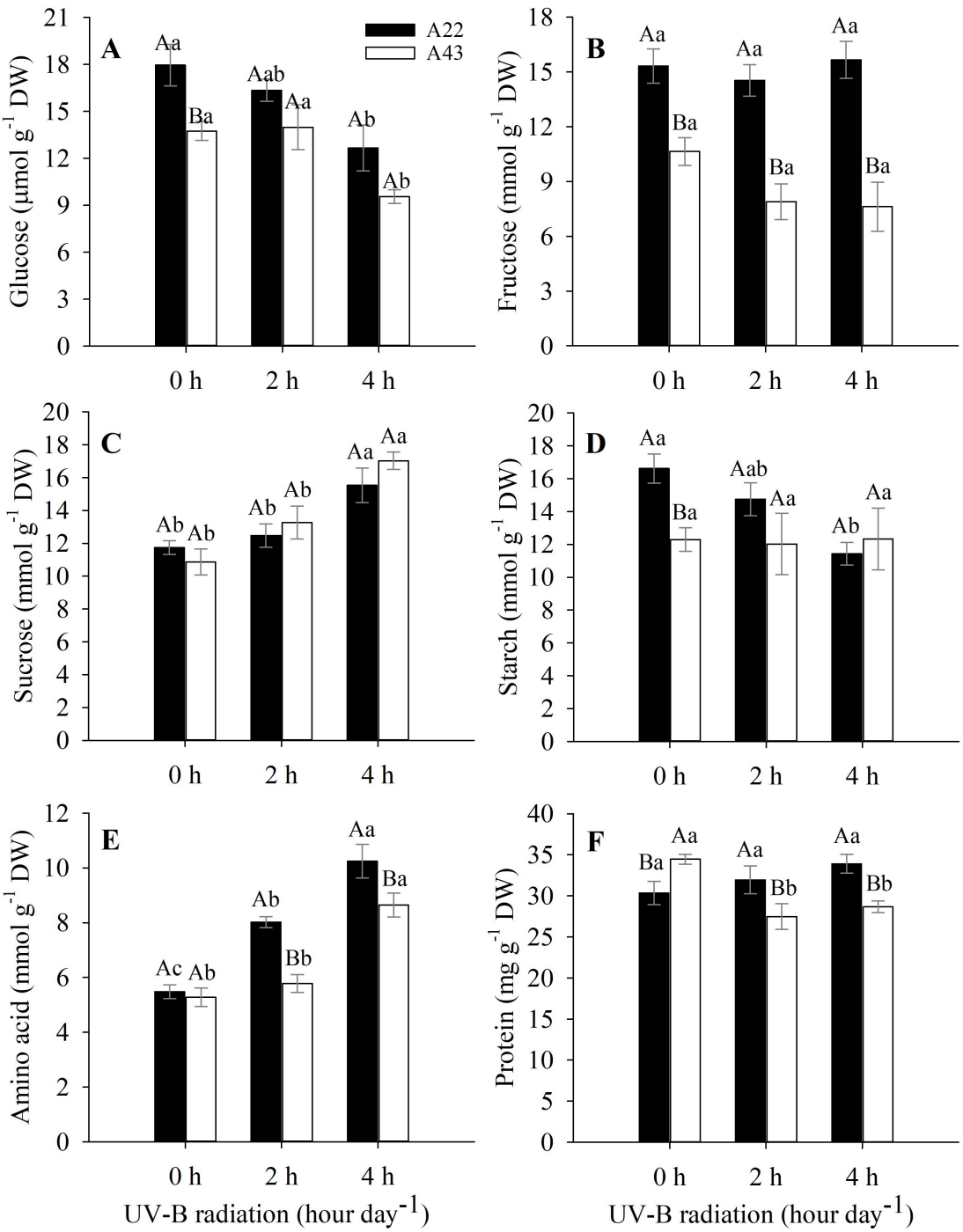

Figure 4. Metabolite levels and protein and starch content in two *P. glomerata* accessions (A22 and A43) grown *in vitro* under different times of UV-B radiations: 0, 2 and 4 h. **A** – Glucose; **B** – Fructose; **C** – Sucrose; **D** – Starch; **E** – Amino acid; and **F** – Protein. Uppercase compares the two accessions at the same time and lowercase compares the same accession at different exposure times. The same uppercase or lowercase letters do not differ at 5% Tukey's test. The bars represent the standard error (n = 4).

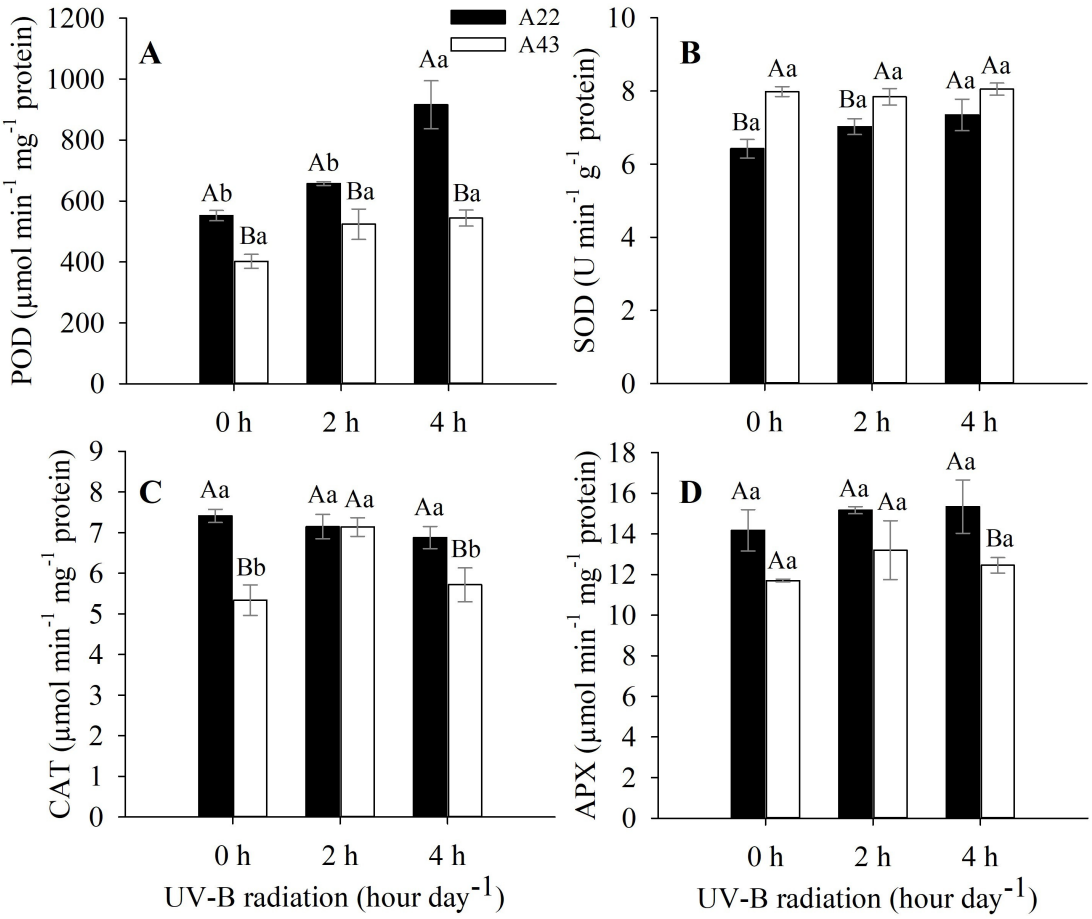

Figure 5. The activities of antioxidant enzymes in two *P. glomerata* accessions (A22 and A43) grown *in vitro* under different times of UV-B radiations: 0, 2 and 4 h. **A** – Peroxidases (POD); **B** – Superoxide dismutase (SOD); **C** – Catalase (CAT); and **D** – Ascorbate peroxidase (APX). Uppercase compares the two accessions at the same time and lowercase compares the same accession at different exposure times. The same uppercase or lowercase letters do not differ at 5% Tukey's test. The bars represent the standard error (n = 4).

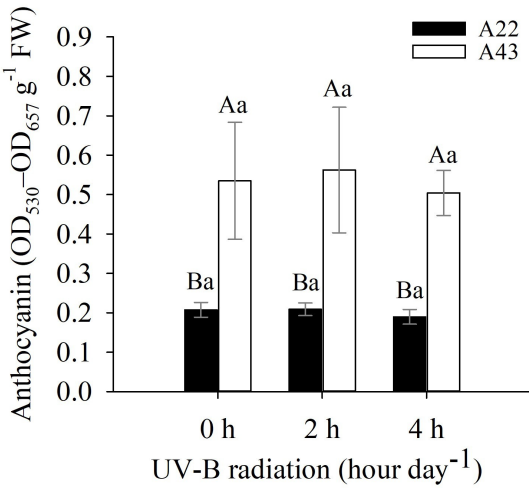

Figure 6. Anthocyanin content in two *P. glomerata* accessions (A22 and A43) grown *in vitro* under different times of UV-B radiations: 0, 2 and 4 h. Uppercase compares the two accessions at the same time and lowercase compares the same accession at different exposure times. The same uppercase or lowercase letters do not differ at 5% Tukey's test. The bars represent the standard error (n = 3).

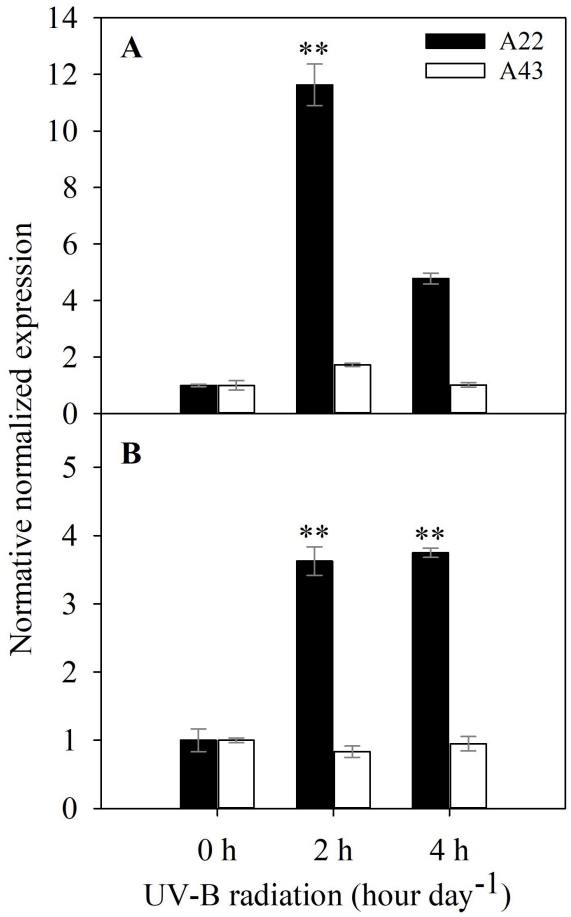

Figure 7. Normalized relative expression of *Spook* and *Phantom* genes in two *P. glomerata* accessions (A22 and A43) grown *in vitro* under different times of UV-B radiations: 0, 2 and 4 h. **A** – *Spook* gene and **B** – *Phantom* gene. Gene expression relative to the control gene *glyceraldehyde-3-phosphate dehydrogenase*. Values represent means ± SD (n = 3), ***P*<0.01 by Dunnett's test.

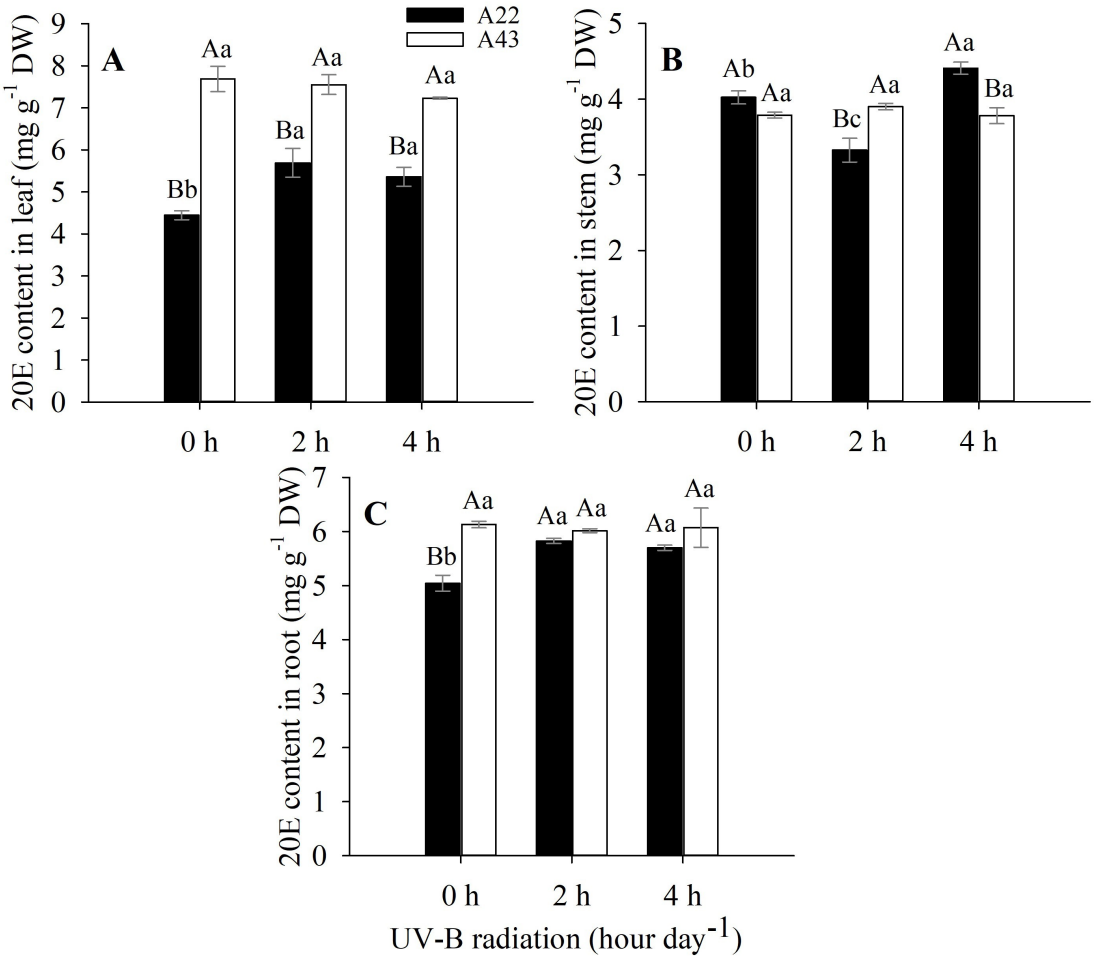

Figure 8. 20-hydroxyecdysone (20E) levels in two *P. glomerata* accessions (A22 and A43) grown *in vitro* under different times of UV-B radiations: 0, 2 and 4 h. 20E content in: **A** – leaf, **B** – stem, and **C** – root. Uppercase compares the two accessions at the same time and lowercase compares the same accession at different exposure times. The same uppercase or lowercase letters do not differ at 5% Tukey's test. The bars represent the standard error (n = 3).

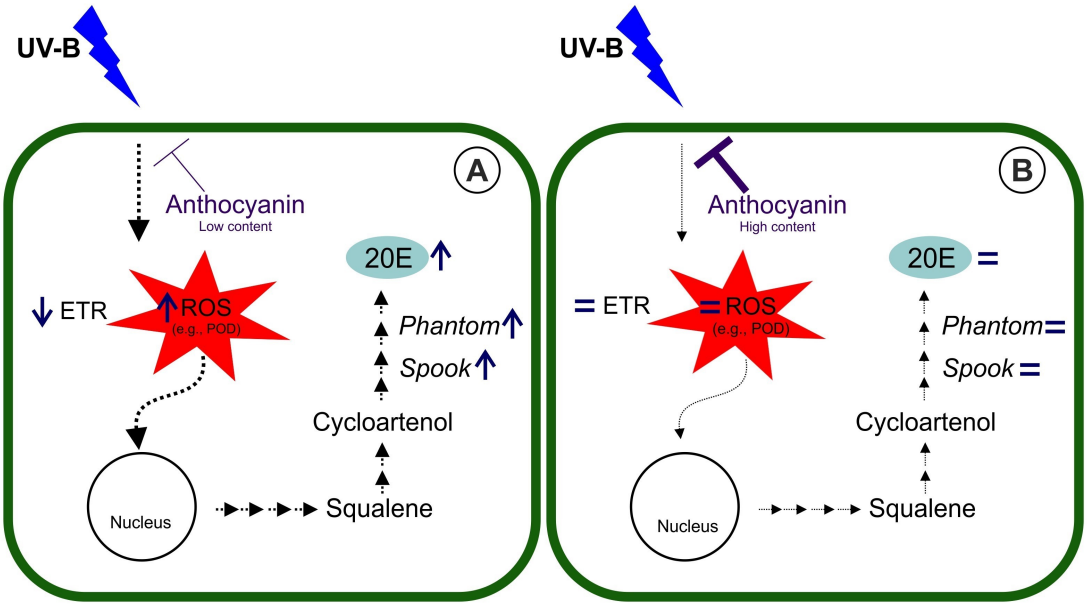

Figure 9. Integrative and schematic view of the main features displayed by *P. glomerata* plants grown *in vitro* under UV-B radiation. **A** – *P. glomerata* plants with low anthocyanin concentration are more responsive to the deleterious effects of UV-B radiation, which promotes a reduction of ETR and an increase in ROS production (estimated by activity of peroxidases) that trigger a cascade of signaling to the cell nucleus, in turn, this causes changes in the secondary metabolism (i.e., upregulation of *Spook* and *Phantom* genes and increase of 20E content). **B** – On the other hand, *P. glomerata* plants with high anthocyanin concentration are less responsive to UV-B radiation and, in turn, there is no strong stress caused by UV-B modulating the gene regulation and increase of 20E content. Positive (black arrows) and negative (purple T-bars) interactions are shown, while blue arrows direction indicates an increase or decrease of the respective metabolite or parameter, and equal sigh indicate no changes.

CONCLUSIONS

The main objective of the present work was to establish a comprehensive perspective of how two abiotic factors – salt stress in plants grown under *ex vitro* conditions and UV-B radiation in plants grown *in vitro* – affect growth performance, physiological features and the regulation of 20-hydroxyecysone (20E) in *P. glomerata*. Even though different experimental approaches were deployed, and each chapter presents an independent discussion focused on the results described, the conclusions below can be extracted from the work:

- Salt stress and UV-B radiation positively modulate 20E biosynthesis.
- Expression of genes (*Spook* and *Phantom*) related to 20E biosynthetic pathways is markedly influenced by salt stress and UV-B radiation.
- Mild salt stress increases 20E concentrations.
- Severe, but not mild, salt stress inhibits growth, ion balance and photosynthetic performance.
- UV-B radiation increases the concentration of 20E in plants with a low concentration of anthocyanin, whereas a high concentration favors the tolerance against UV-B radiation, that in turn, mitigates the UV-B stress and the biochemical response that leads to an increase of 20E.
- Plants with a low concentration of anthocyanin are more damaged by UV-B radiation (i.e., they display a lower growth and the chlorophyll *a* fluorescence is affected) than plants with a high concentration.

Notably, our results are a contribution to a better understanding of the relationship between salt stress and UV-B radiation and the regulation of the production of 20E, magnifying the bases for further studies intended to induce the increase of this secondary metabolite in plants grown *ex vitro* and *in vitro*.